Final analysis report : Imbalance Mach-Zender Interferometer

Guy Yehudian (Username: guyyehudian)

(fork name: guykibalano-bit)

- ## Introduction:

Integrated silicon photonics enable implementation of compact optical circuits, which use light to preform various tasks like electronics in high-speed rate. such as computing, data transferring and modulation.it can be used in various applications such telecommunications, data center, quantum computers, bio-medical diagnostics and research and more.

One of the advantages of photonics is that it has similar concepts as in integrated electrical circuits. The same CMOS foundry technology, in particular old technology, can be used to fabricate integrated photonics circuits.

This design concentrate in IMZI optic device (Imbalanced Mach-Zender Interferometer), which can be used to extract silicon strip waveguide parameters such as FSR (Free-Spectral-Range) and group index.

- ## Theory

An Imbalanced Mach-Zender Interferometer (IMZI) is an optical device, which uses beam interference to apply relative phase shift between two light beams travelling along two different wave guides paths. It consists of 2 wave guides with different length (ΔL=L1 - L2), which control the output light intensity. The MZI transfer function between output light intensity (*Io*) and input light intensity (*Ii*) is:

$$\frac{\boldsymbol{Io}}{\boldsymbol{Ii}} = \frac{\mathbf{1}}{\mathbf{4}} * \left| \mathbf{1} + \mathbf{e}^{-i\boldsymbol{\beta}\Delta\boldsymbol{L}} \right|^{\mathbf{2}}$$

in ideal case of no loss, MZI Transfer function reduced to:

$$\frac{\boldsymbol{Io}}{\boldsymbol{Ii}} = \frac{\mathbf{1}}{\mathbf{2}} * (\mathbf{1} + \mathbf{cos}(\boldsymbol{\beta} * \Delta\boldsymbol{L}))$$

Where β is called "propagation constant" and it depends in effective index of the wave guide:

$$\boldsymbol{\beta} = \frac{2*\pi*Neff}{\lambda} + i\frac{\alpha}{2}$$

Where α is “propagation loss coefficient”, typically varied between 1-10db/cm for Silicon waveguides. in case of no loss, it can be ignored.

The transmission spectrum of MZI is a periodic function, which depends on wavelength, with maximum and minimum periodic points. A Free Spectral Range (“FSR”) is the length between two maximum points. “FSR” parameter can be calculated by the following equation:

$$\boldsymbol{FSR} = \frac{\boldsymbol{\lambda^2}}{\boldsymbol{Ng} * \boldsymbol{\Delta L}}$$

Where Ng is a “group index” parameter of the wave guide. In this design, we will compare wave guide simulation with experimentally extracted group index from experiments. The calculated group index can be found using FSR equation:

$$\boldsymbol{Ng} = \frac{\boldsymbol{\lambda^2}}{\boldsymbol{FSR} * \boldsymbol{\Delta L}}$$

- ## Modeling and Simulation

The design includes 5 IMZI cells and a de-embedding structure of 2 grating couplers connected for insertion loss calibration. The first 4 IMZI cells consist of Y-branch splitter/combiner with wave guides configured to various length difference (ΔL). The last IMZI consist of Broad band direct coupler splitter/combiner with ΔL like IMZI 3 to extract the differences between two MZI configuration. The simulated FSR decreases while wave guide length difference increases.

The “GC_PAIR_0” (de-embedding GC structure) cell will be used to measure grating coupler insertion loss for calibration.

The waveguides parameters used for IMZI design are:

Thickness: 220nm

Width:500nm

Length: Different length according to IMZI cells:

Layout cell name	L1 (um)	L2 (um)	ΔL (um)	Calculated FSR (nm)	Note
IMZI_Y-Branch_1	140	178	38	15	*Ng approximate to 4.2 for FSR calculations
IMZI_Y_Branch_2	140	197	57	10	
IMZI_Y_Branch_3	140	254	114	5	
IMZI_Y_Branch_4	140	369	229	2.5	
IMZI_BDC_SP_5	**140**	**254**	**114**	**5**	***Same parameters as IMZI 3**

Table 1: Fabricated MZIs ΔL / FSR (predicted)

The fabricated MZIs layout schematics are illustrated in following figure:

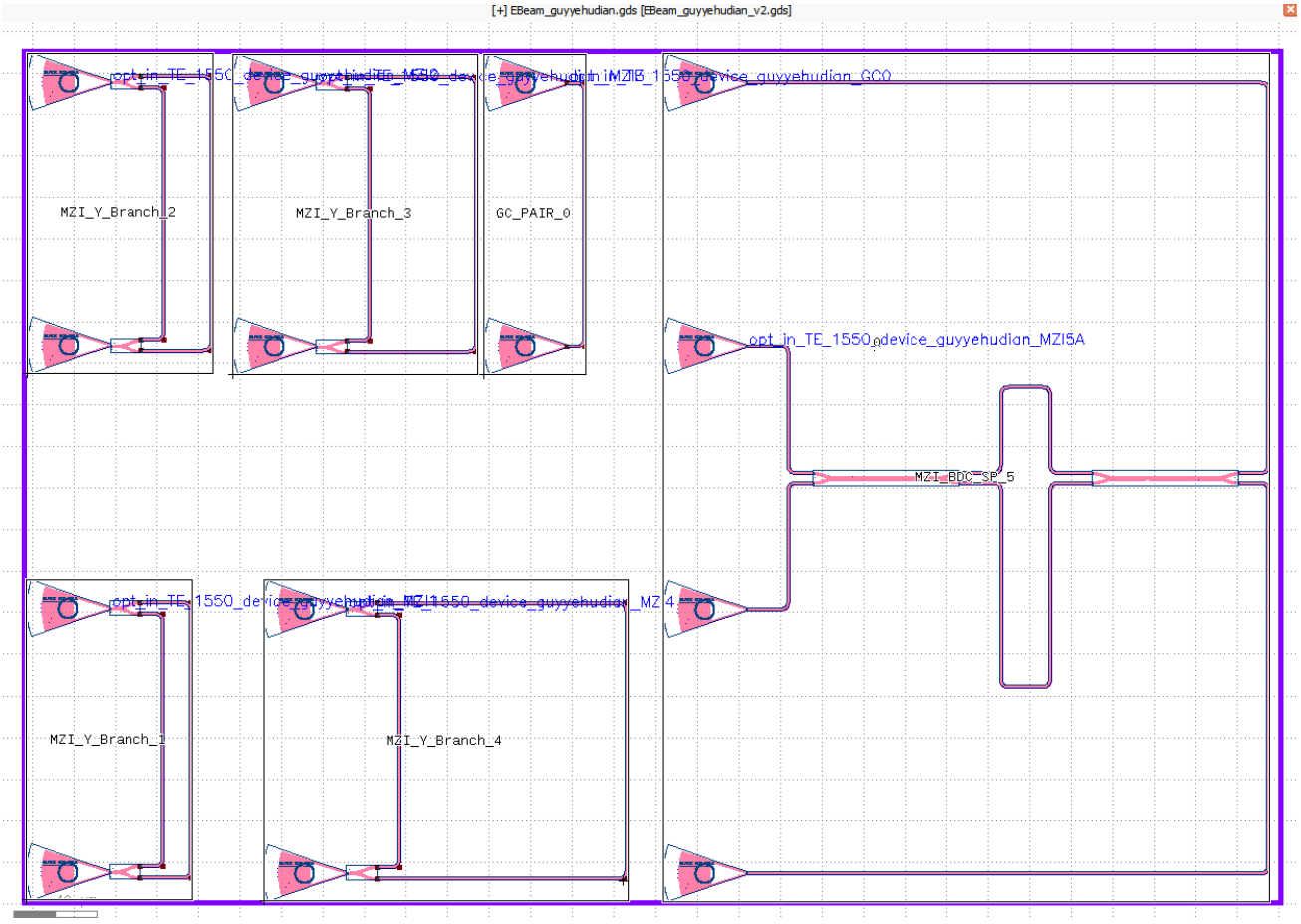

Figure 1: MZIs Layout view

Corner analysis simulation and waveguide modelling

To take into account, the manufacturing variation in waveguide geometry, we simulate using Lumbrical MODE tool different corners of waveguide width and thickness to generate a "waveguide compact model" for each corner. The compact model is a Tylor expansion, which model the dependence of effective index around center wavelength ($\lambda 0$):

$$\mathbf{Neff(\lambda) = n1 + n2*(\lambda - \lambda 0) + n3*(\lambda - \lambda 0)^2}$$

from Tylor coefficients n1, n2 and n3, we derived the waveguide parameters for each corner - effective index ("Neff"), group index("Ng") and desperation ("D"):

Neff = n1;

Ng = n1 – n2*λ0

D = -2*λ0*n3/c

After generating these parameters, we can simulate MZI circuits, using Lumerical interconnect tool and compare simulation results to experimental measurements.

The following tables show MODE simulation results for each width/thickness corner. Notice that effective index **increases** with both width and thickness **increasing**, as expected. The effective index first derivative (n2 coefficient) **decreases** with both width and thickness increasing, however n2 decreasing dominates by width increasing, which leads to variation in group index (decreasing) and FSR (increasing) with width variations mainly.

(Note: To compare with experimental results, I used 5 bold corners only (4 extreme corners and 1 nominal)).

Width (nm)		Thickness (nm)		
		215.3	220	223.1
470	N1	**2.37245**	2.39159	**2.40388**
	N2	**-1.21322**	-1.20744	**-1.19885**
	N3	**-3.41E-02**	-4.65E-02	**-5.28E-02**
500	N1	2.42755	**2.44682**	2.45799
	N2	-1.14008	**-1.13339**	-1.12615
	N3	-3.43E-02	**-4.39E-02**	-4.86E-02
510	N1	**2.44161**	2.46076	**2.47221**
	N2	**-1.12129**	-1.11459	**-1.10681**
	N3	**-3.33E-02**	-4.23E-02	**-4.65E-02**

Table 2: MODE Simulation results - "compact model" coefficient n1, n2, n3

Width (nm)		Thickness (nm)		
		215.3	220	223.1
470	Neff	**2.37245**	2.39159	**2.40388**
	Ng	**4.25295**	4.26313	**4.26209**
	D [s/m²]	**3.52E-10**	4.81E-10	**5.46E-10**
500	Neff	2.42755	**2.44682**	2.45799
	Ng	4.19468	**4.20358**	4.20353
	D [s/m^2]	3.55E-10	**4.54E-10**	5.03E-10
510	Neff	**2.44161**	2.46076	**2.47221**
	Ng	**4.1796**	4.18839	**4.18777**
	D [s/m^2]	**3.44E-10**	4.38E-10	**4.81E-10**

Table 3: MODE simulation results - Waveguide parameters

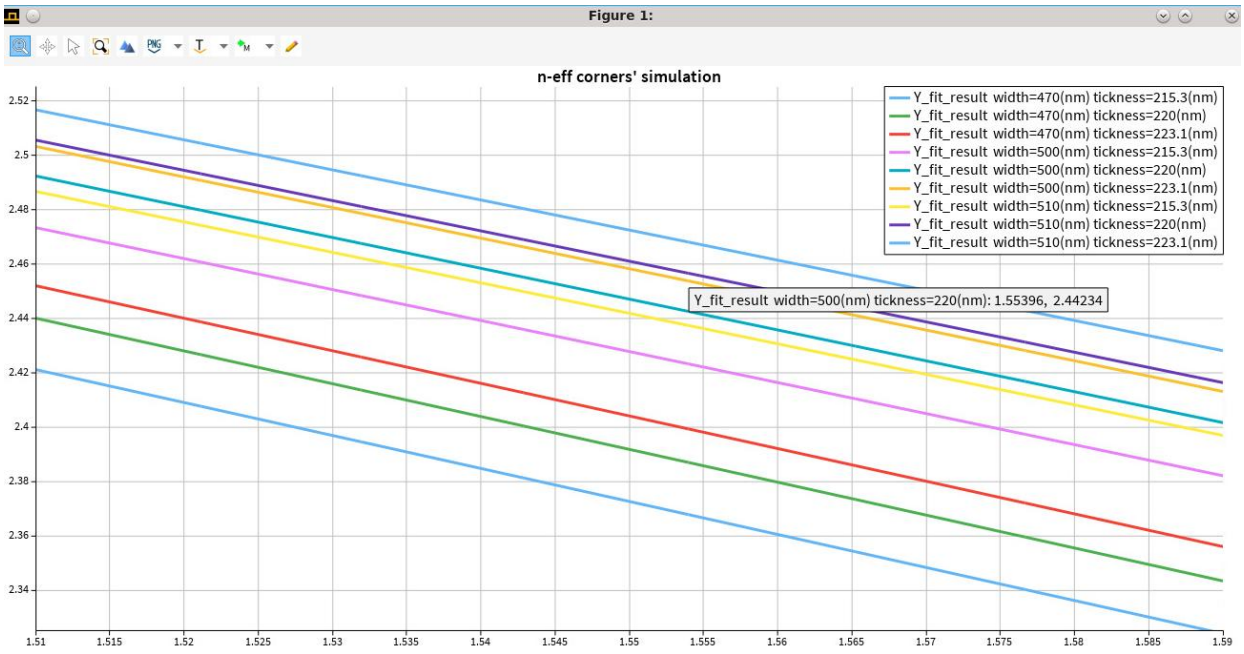

Figure 2: MODE Simulation results - Effective index for each corner

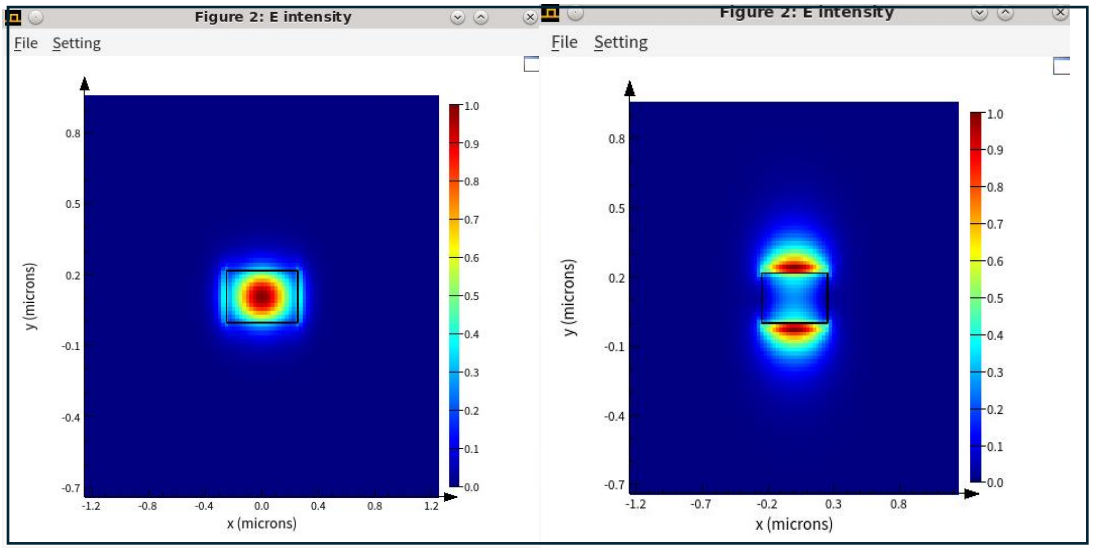

Figure 3: MODE Simulation results – MODE Profile result for first mode TE (Left picture) and second mode TM (Right picture) for wavelength 1550nm typical corner (Width=500nm, Thickness=220nm)

MZIs interconnect corner simulation results

After generating the wave guide parameters using our waveguide compact model, we can simulate our MZIs using interconnect component called “straight waveguide”. These waveguide components updated with effective index, group index, dispersion and L1/L2 lengths parameters corresponding to specific corners and MZI. The simulation results data are collected to text files in order to compare it to experimental results after fabrication. The following figures shows the MZI schematics for both types of fabricated MZIs:

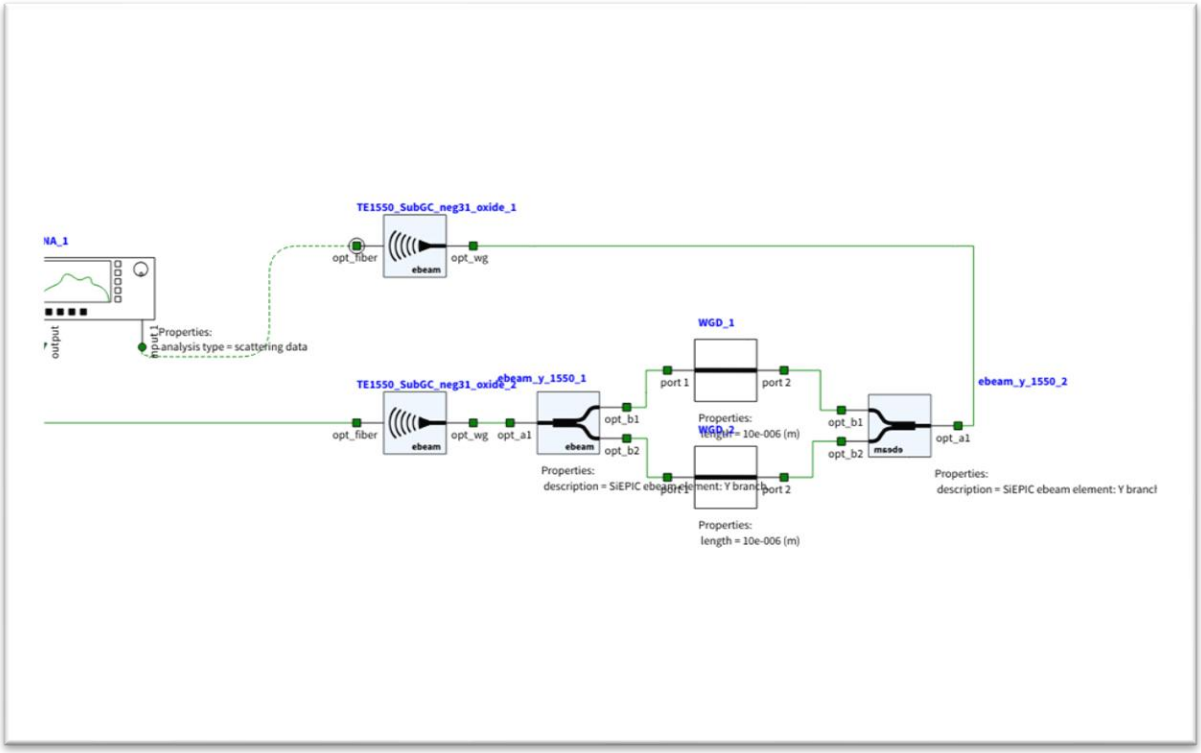

Figure 4: Simulation schematic for MZI 1 – 4 (MZI with Y-Branch components)

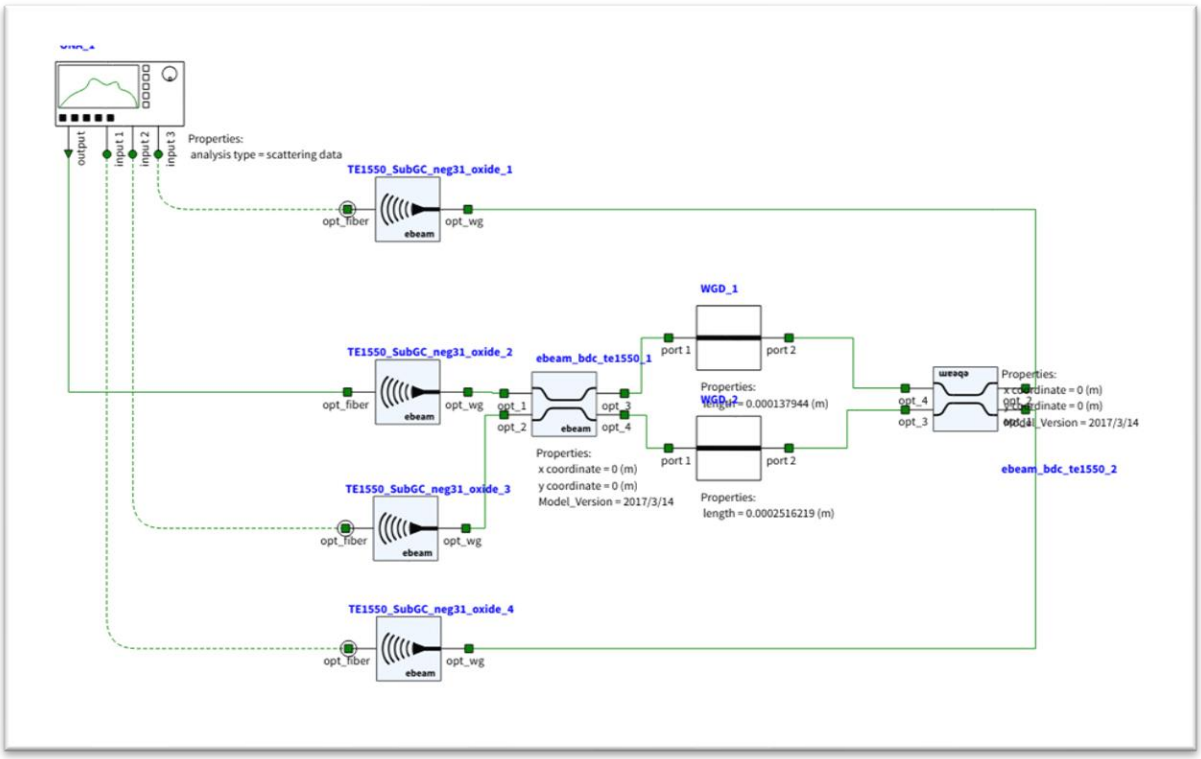

Figure 5: Simulation schematic for MZI 5 (MZI with bdc splitter components)

Transmission spectrum and FSR simulation results

The following figures describes the gain spectrum and FSR simulation results corresponding to various IMZI. The FSR results are as expected and align with table 1:

I

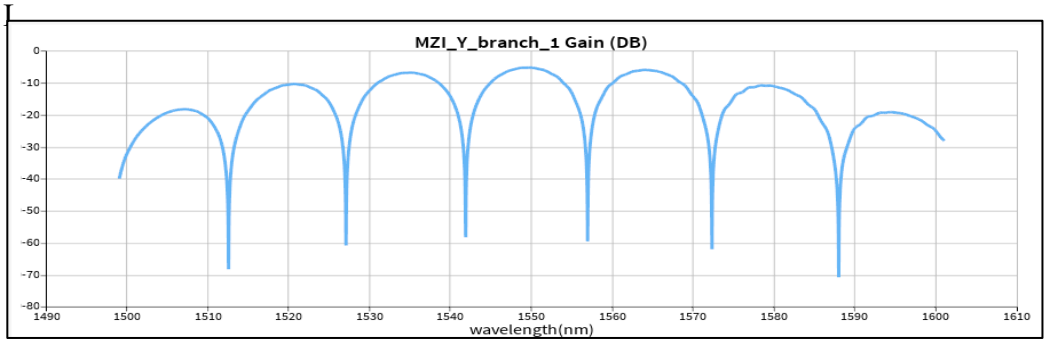

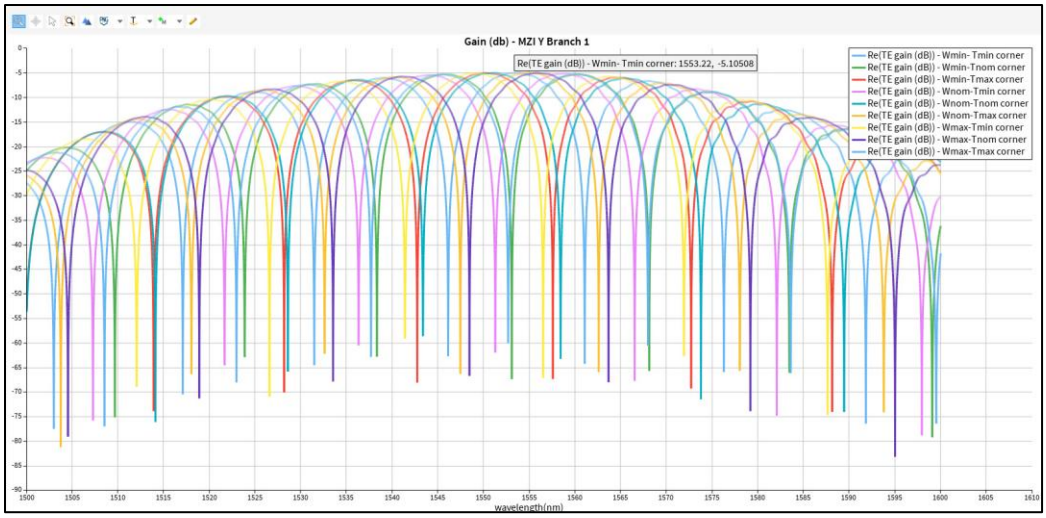

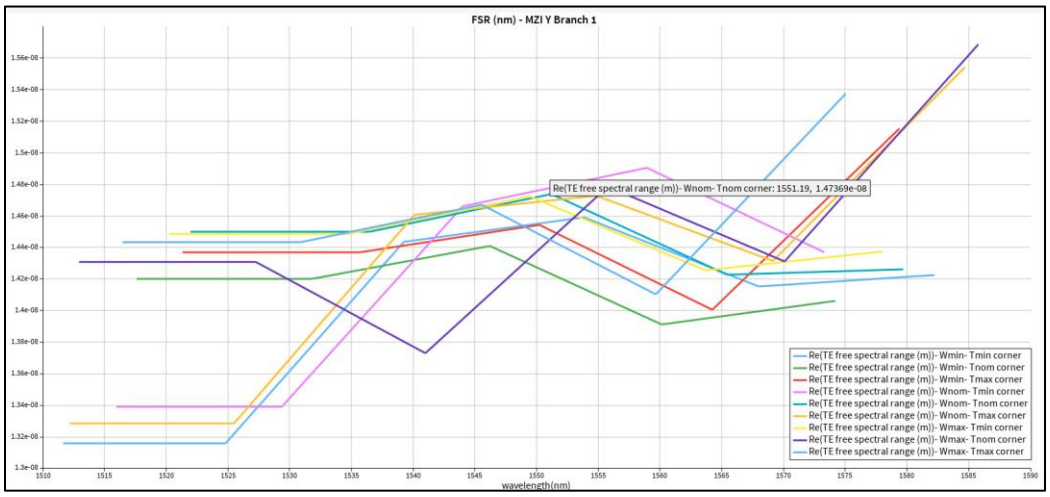

Figure 6: MZI 1 ΔL = 38um (a. Transmission for nominal corner only (w=500nm, T=220nm) (Top), b. Transmission for all corners (middle) c. FSR for all corners (Bottom))

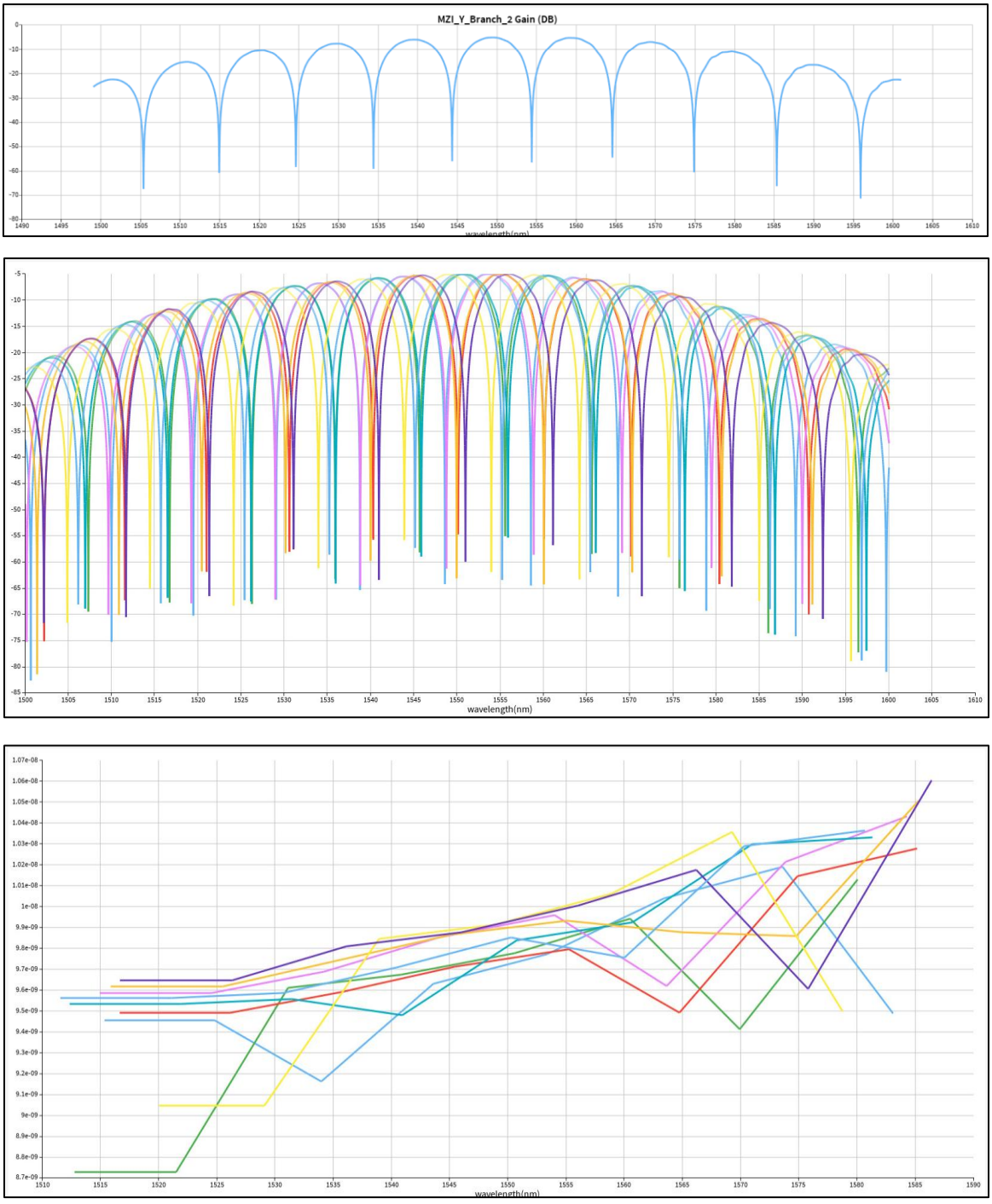

Figure 7: MZI 2 ΔL = 57um (a. Transmission for nominal corner only (w=500nm, T=220nm) (Top), b. Transmission for all corners (middle) c. FSR for all corners (Bottom))

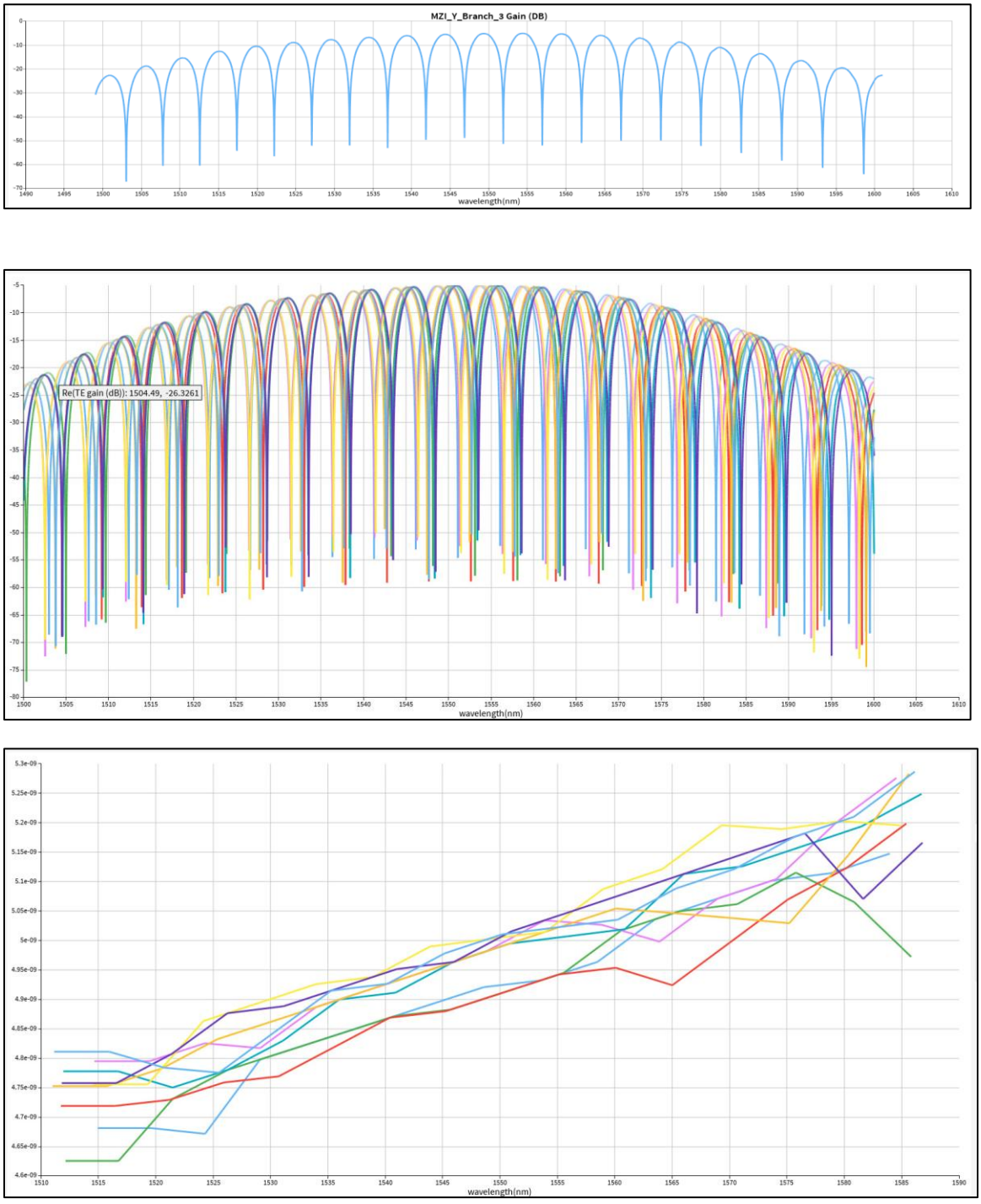

Figure 8: MZI 3 ΔL = 114um (a. Transmission for nominal corner only (w=500nm, T=220nm) (Top), b. Transmission for all corners (middle) c. FSR for all corners (Bottom))

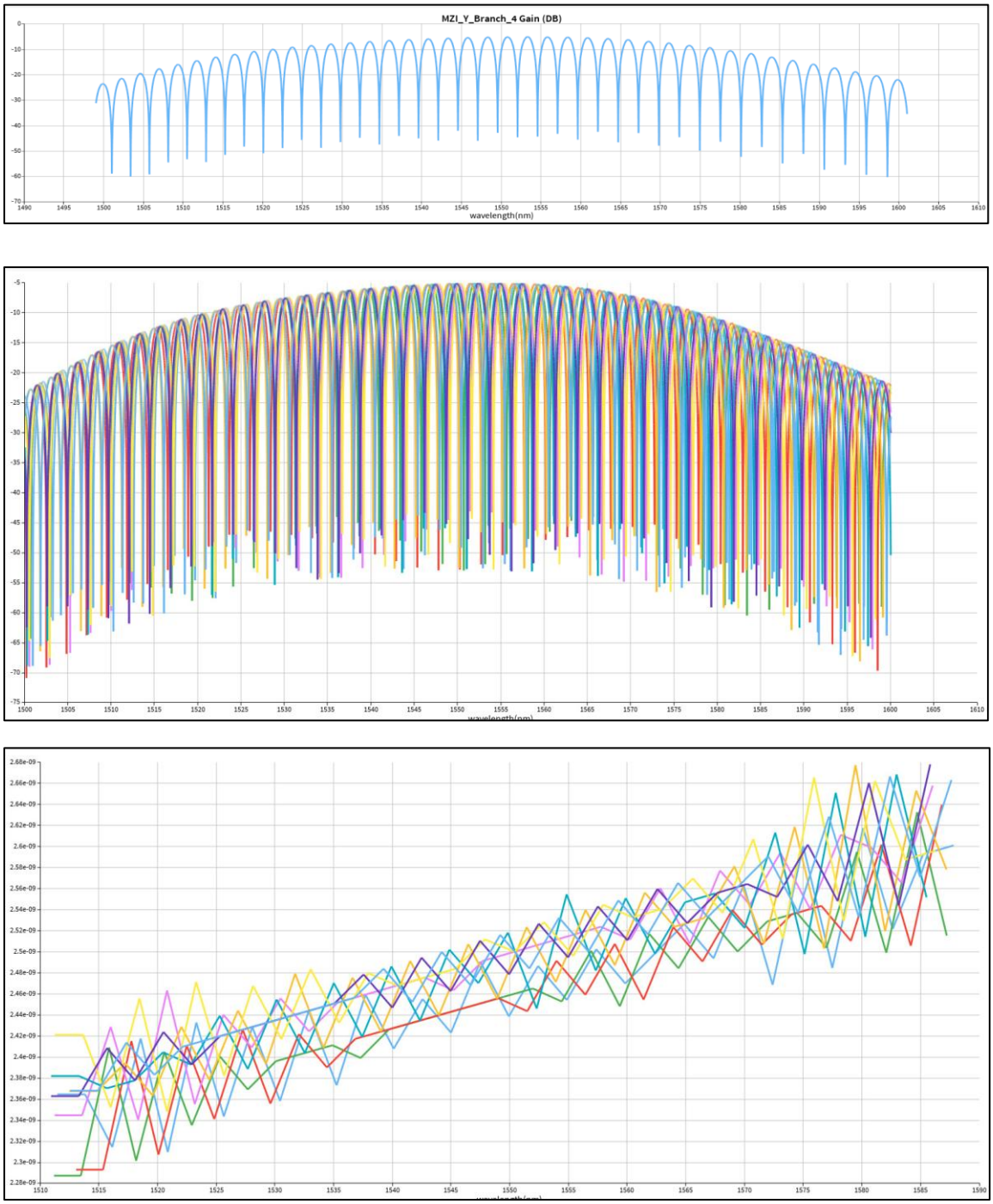

Figure 9: MZI 4 ΔL = 229um (a. Transmission for nominal corner only (w=500nm, T=220nm) (Top), b. Transmission for all corners (middle) c. FSR for all corners (Bottom))

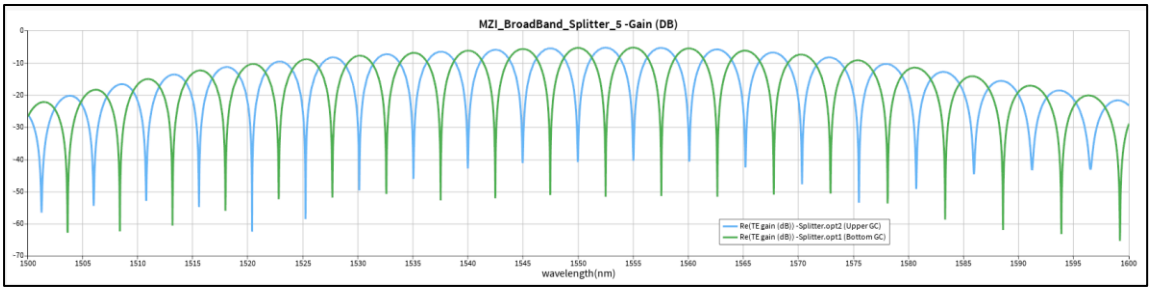

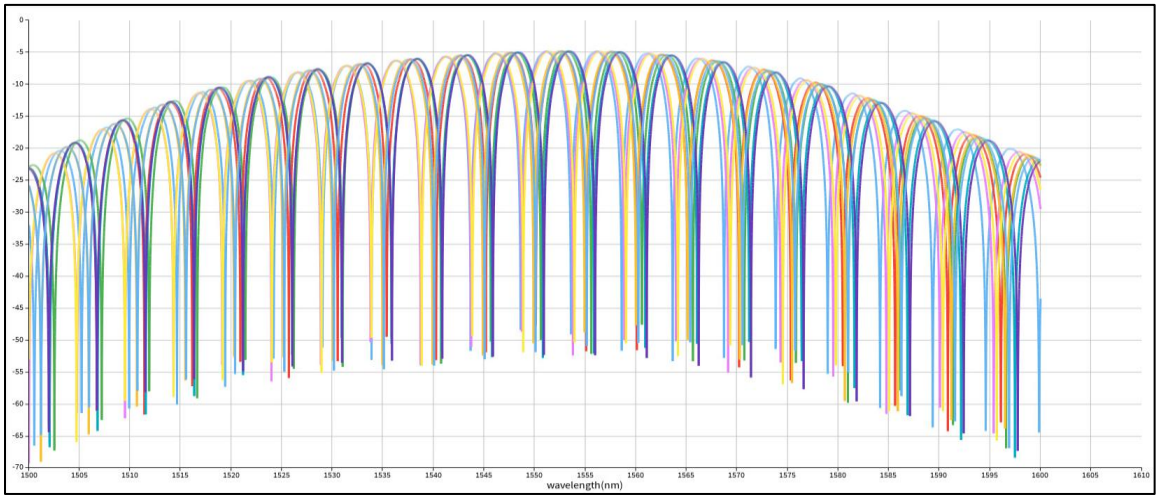

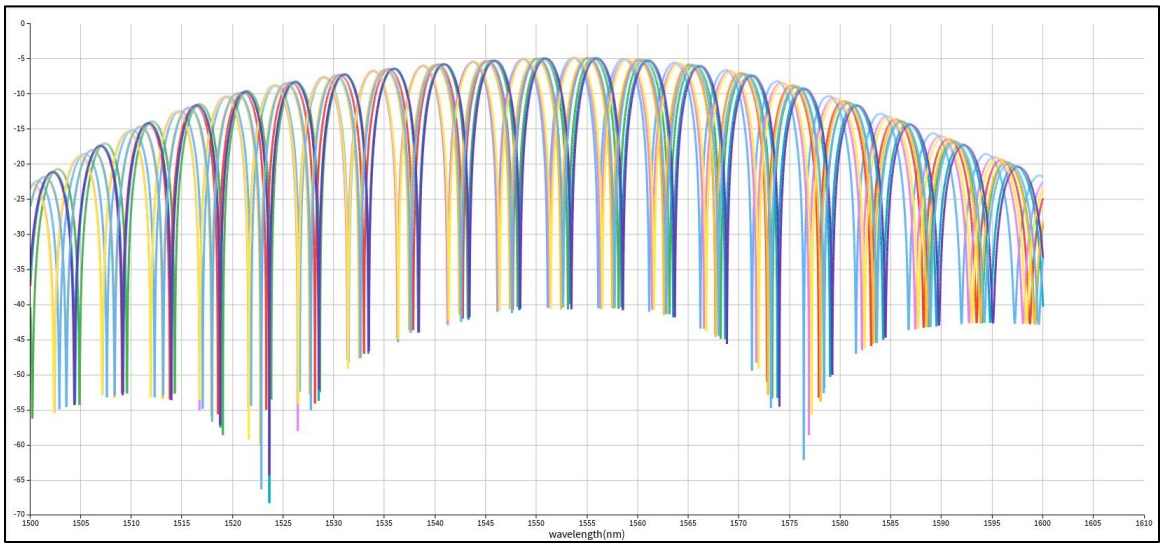

Figure 10: MZI 5 ΔL = 114um (a. Transmission for nominal corner only (w=500nm, T=220nm) both grating coupler on same graph (Top), b. Transmission for all corners (middle) Upper GC (input 3) c. Transmission for all corners (Bottom) Bottom GC (input 1)

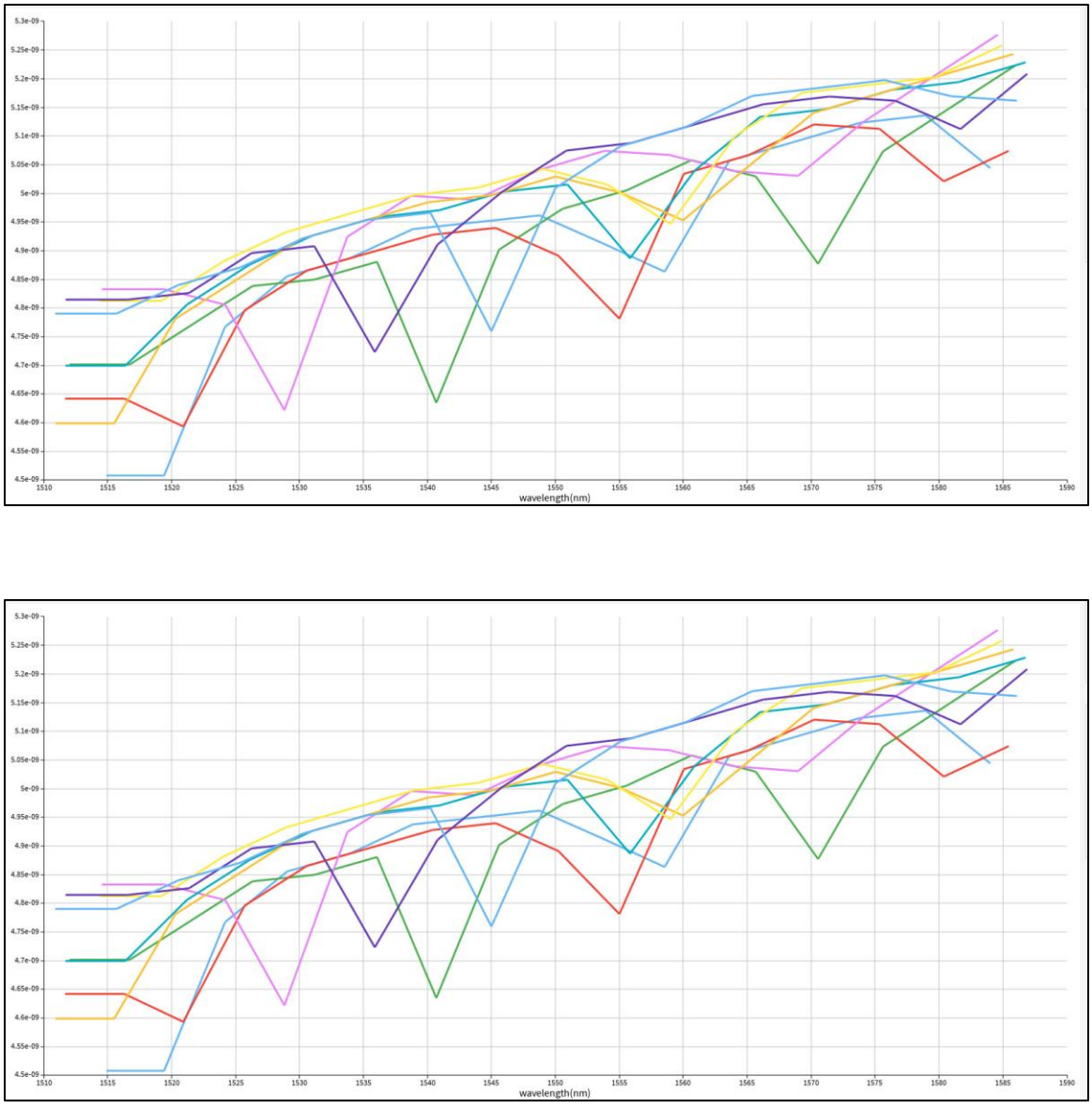

Figure 11: MZI 5 ΔL = 114um (a. FSR for all corners Upper GC (input 3) (Top) b. FSR for all corners Bottom GC (input 1) (Bottom)

Experimental results data analysis

To estimate fabricated MZIs designs, we extract waveguide parameters from experimental data and generate MZI transfer model using curve fitting method. The MZI fitting model and parameters extracted from experimental are compared to simulation to show the matching between simulation and experimental results.

The most important objective is to extract the group index from the experimental measurements and compare it to corners simulation results.

The analysis method includes the following steps:

- **<u>Experimental data analysis:</u>**
  1. **Baseline correction for experimental data -** This correction eliminates the baseline shape of the grating coupler. There are two methods for baseline correction:
     a. **Loopback calibration using gating-coupler pair (Figure 12)** – This method was used for MZI 1. In this method, we perform a polynomial fitting on GC pair results and subtract the curve fit from MZI amplitude experimental results.
     b. **Polynomial fitting correction (Figure 13) –** This method was used for MZI 2 – 5. In this method we preform a polynomial fitting on MZI experimental amplitude results and subtract it.
  2. **Find FSR using autocorrelation of experimental amplitude (Figure 14)** - Extract group index around λ0 ("Average ng" parameter) and n1, n2, n3 waveguide compact model coefficient to generate MZI model.
  3. **Repeat autocorrelation between experimental amplitude and MZI model (Figure 15)** - Eliminate the shift between experimental and model amplitudes. Update MZI model effective index parameter.
  4. **Curve fitting using least-square fitting to updated MZI model of experimental data (Figure 15)** – Extract group index as a function of wavelength for experimental data.
- **<u>Simulation data analysis:</u>**
  5. Repeat previous steps 1 – 4 on simulation data for each corner separately and extract group index as a function of wavelength for each simulated corner.

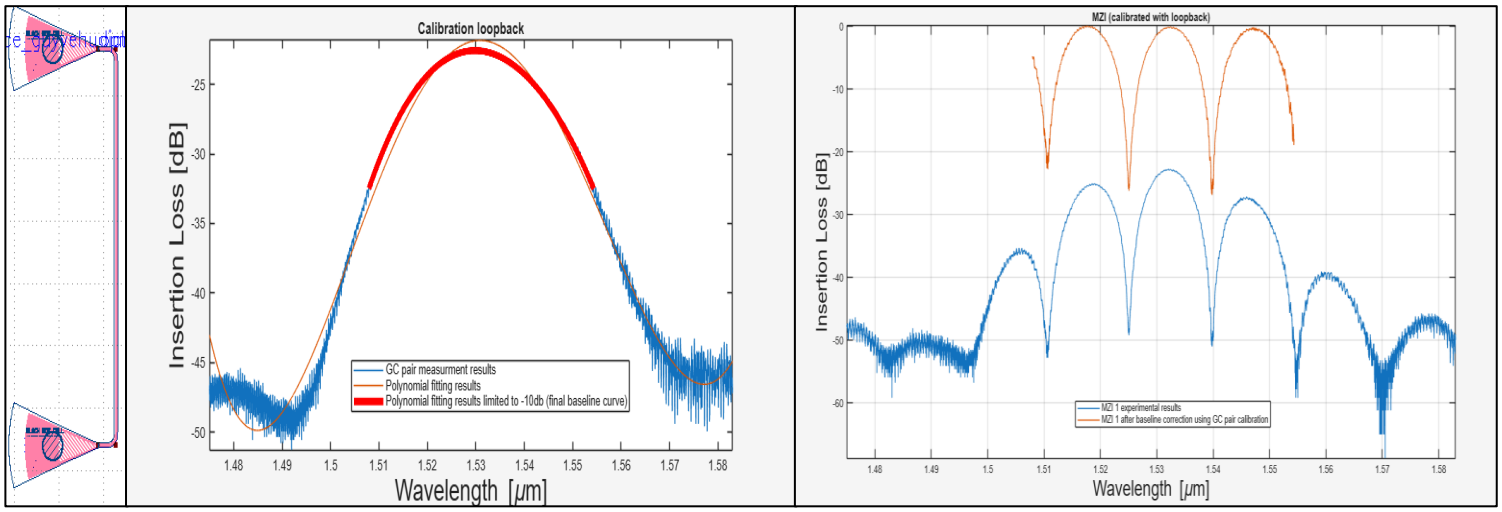

Figure 12: Loop-back calibration method (From left to right)– (a.) GC pair schematic (b.) polynomial fitting curve (c.) MZI1 experimental results Vs. MZI1 after base-line correction using loopback calibration

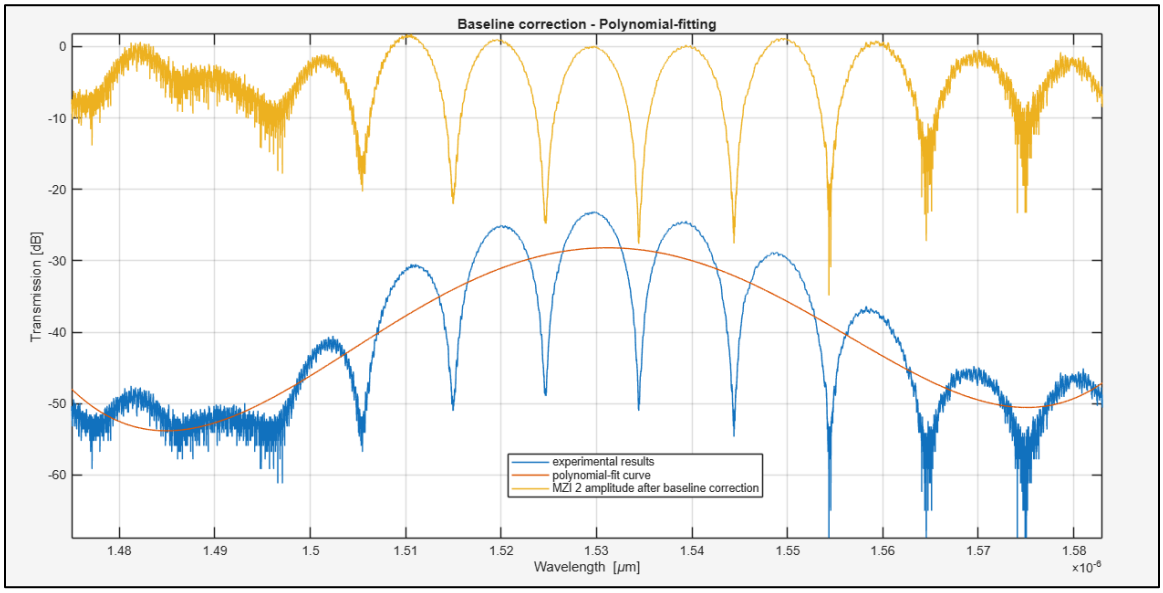

Figure 13: MZI 2 amplitude base line correction using polynomial fitting

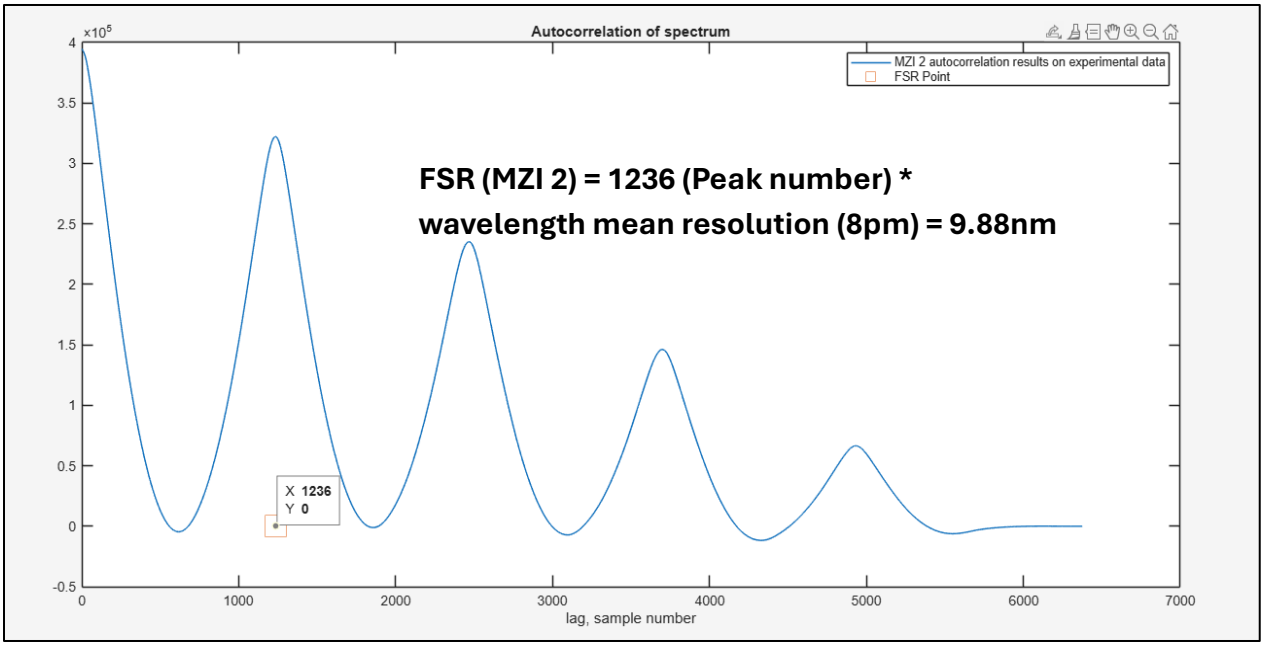

Figure 14: MZI 2 experimental data autocorrelation results

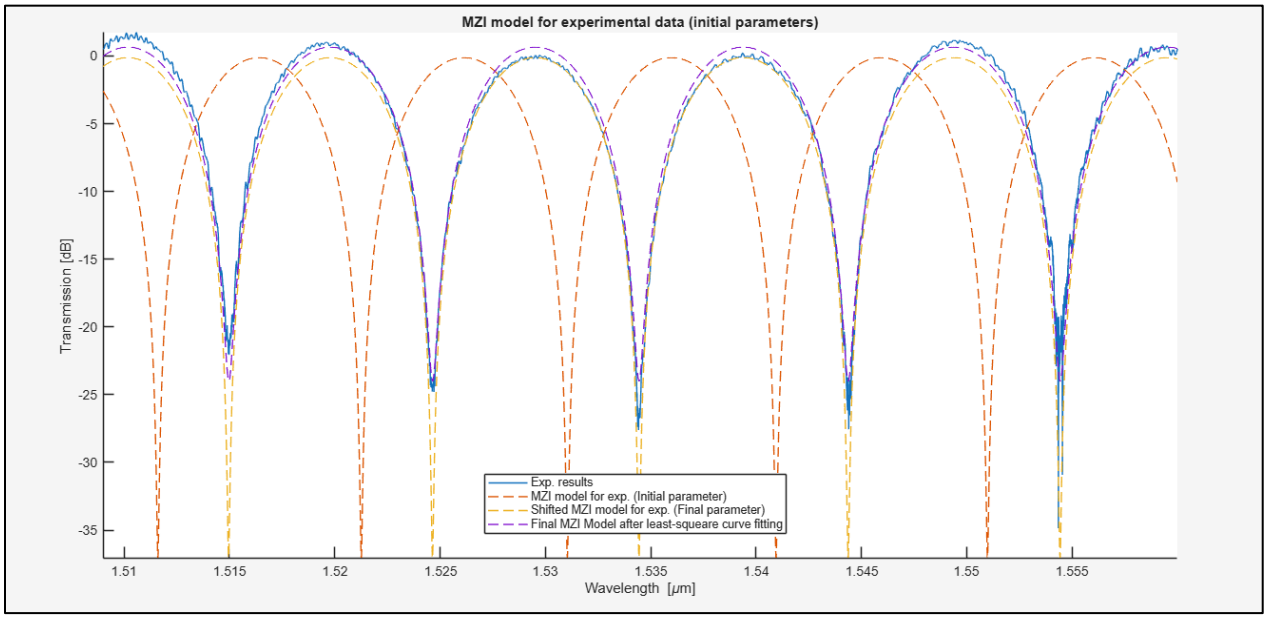

Figure 15: MZI 2 Model extracted from experimental results (corresponding to steps 2 – 4)

Experimental data results Vs. corner simulation

The following waveforms shows simulation results Vs. experimental results for each MZI. The figures are in the following order:

1. Overlay simulation (Nominal) data and experimental data – Shows starting point of data analysis.
    a. Higher GC loss in experimental compared to simulation. (~22db Vs. ~5db).
    b. Noise on spectrum sides in experimental data.
    c. Laser wave-length shift in experimental compared to simulation. (1.53um Vs 1.55um).

2. Overlay plot of MZI Transfer model after curve fitting for both simulation data and experimental data (Nominal case). Eliminates noise and GC loss to align experimental and simulation spectrums.

3. Overlay plot of group index for simulation data and experimental data (Nominal).

4. Overlay plot of group index for simulation data and experimental data (All corners).

MZI 1 - (ΔL = 38um, Predicted FSR (calculated) = 15nm)

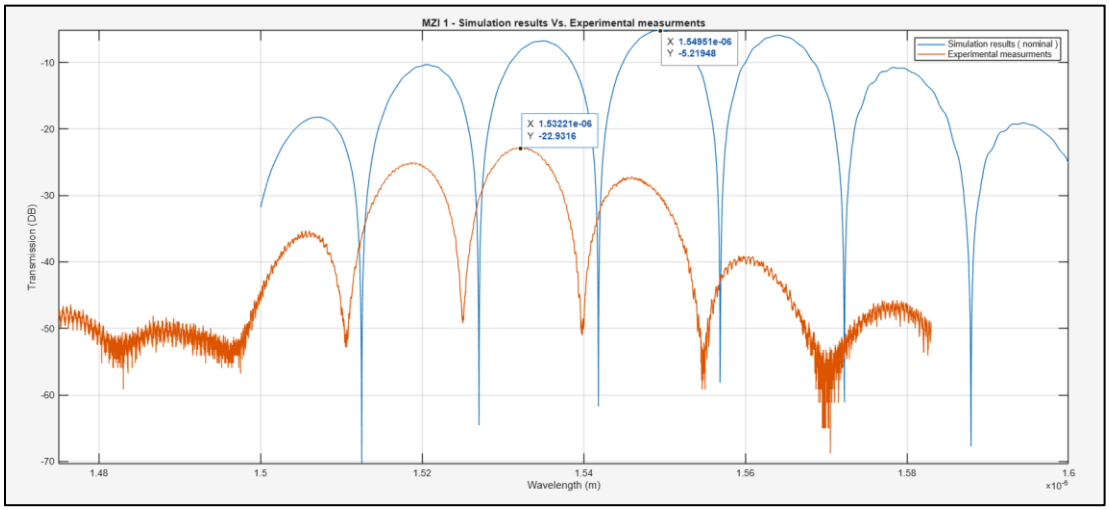

Figure 16 - 1: MZI 1 – Simulation (Nominal) Vs. Experimental data

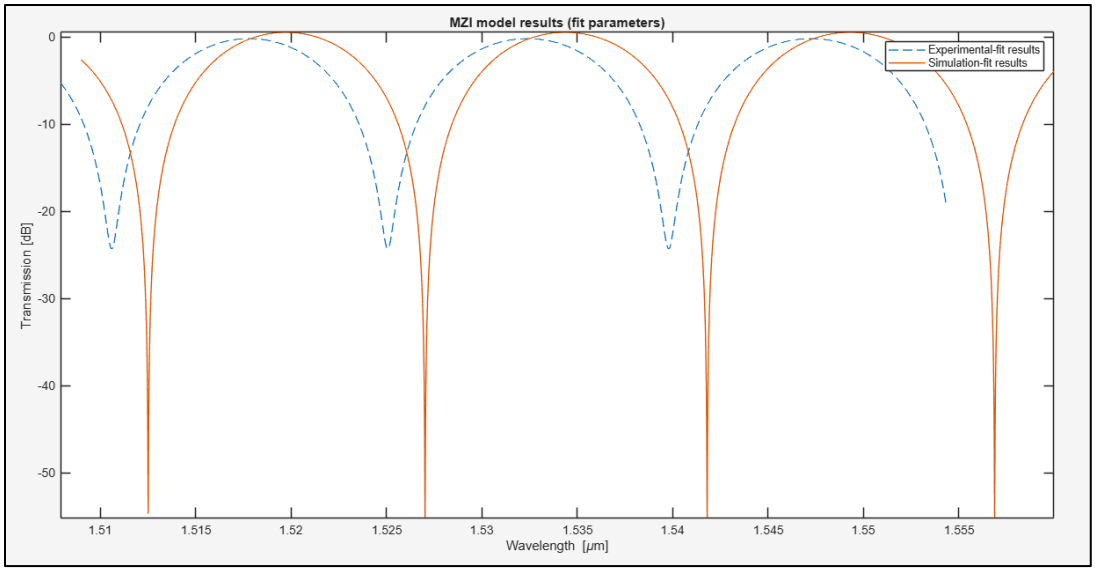

Figure 16 - 2: MZI 1 - MZI Transfer model fit – Simulation Vs. Experimental (Nominal corner only)

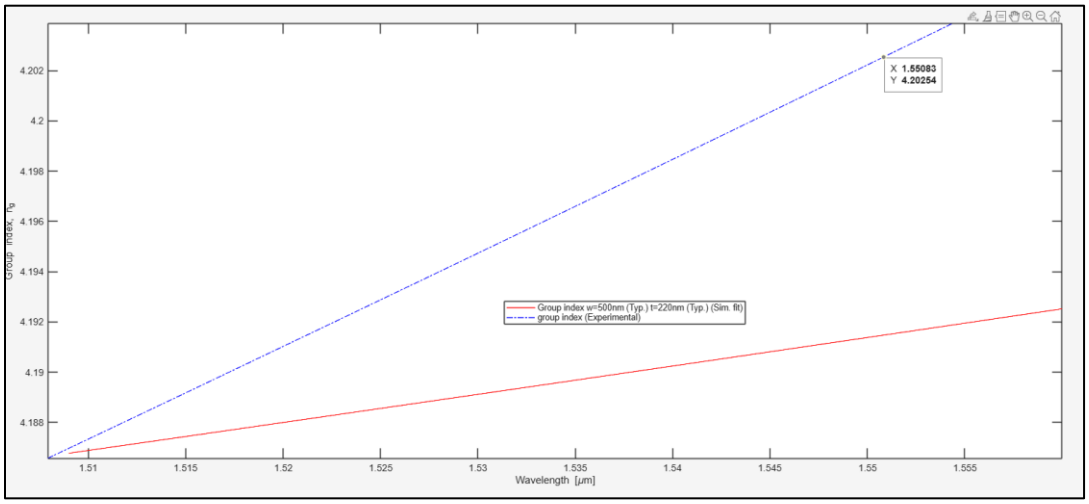

Figure 16 - 3: MZI 1 – Group index – Simulation Vs. Experimental (Nominal corner only)

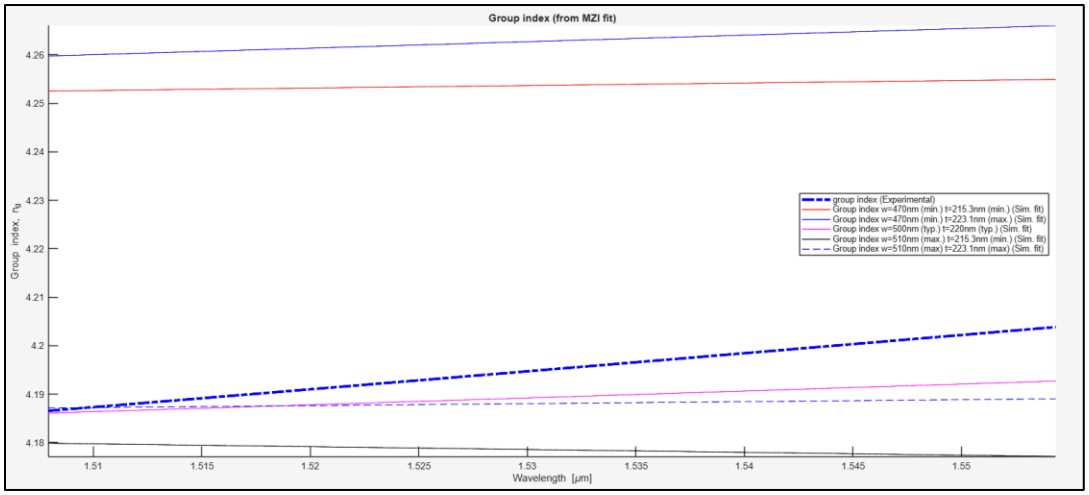

Figure 16 - 4: MZI 1 – Group index – Simulation Vs. Experimental (All corners)

MZI 2 - (ΔL = 57um, Predicted FSR (calculated) = 10nm)

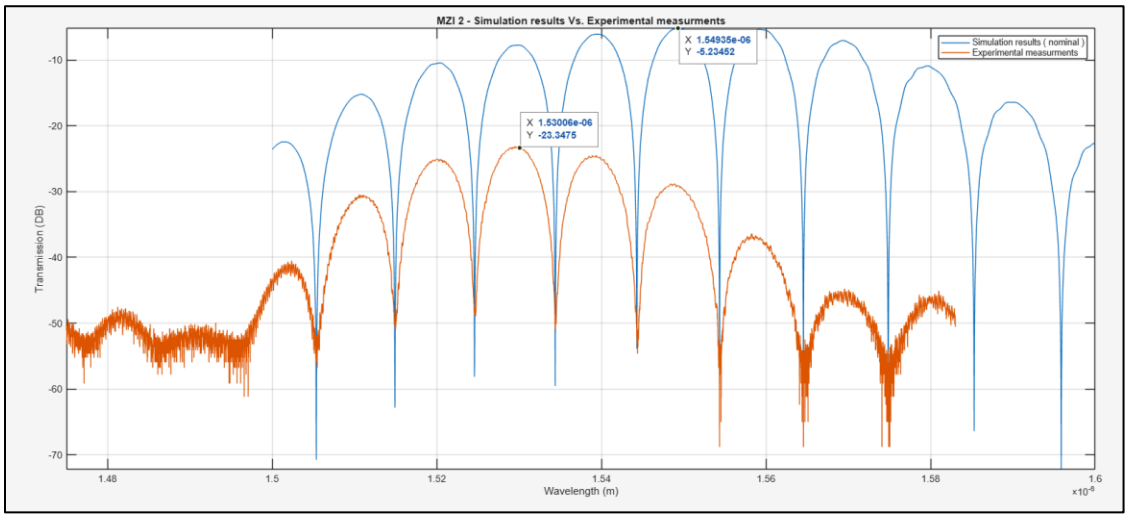

Figure 17 - 1: MZI 2 – Simulation (Nominal) Vs. Experimental data

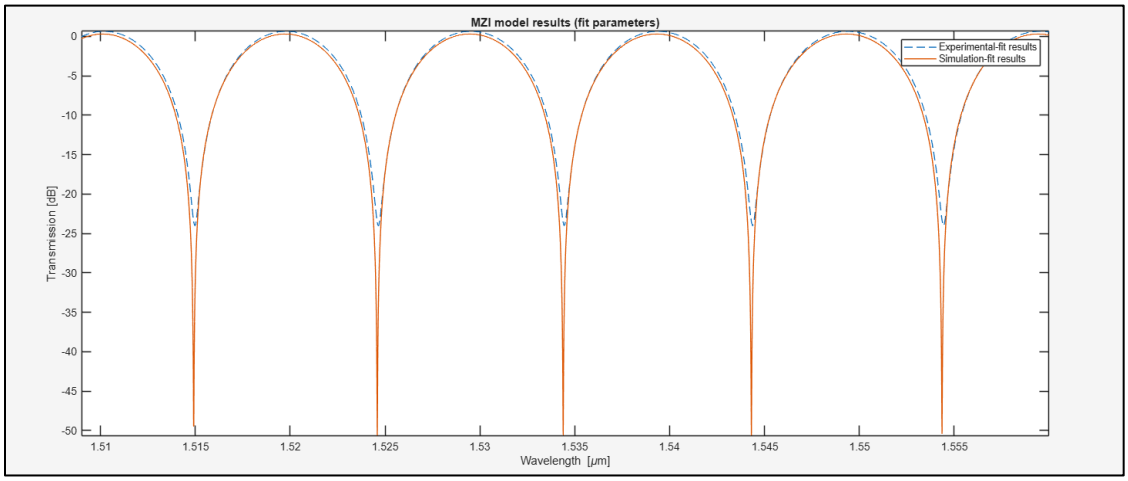

Figure 17 - 2: MZI 2 - MZI Transfer model fit – Simulation Vs. Experimental (Nominal corner only)

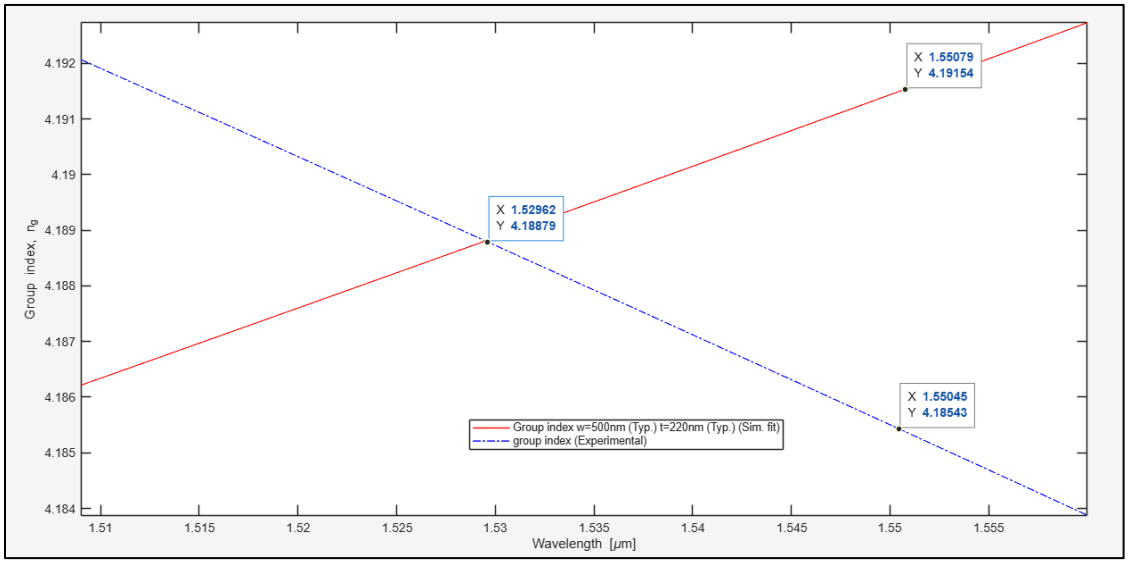

Figure 17 - 3: MZI 2 – Group index – Simulation Vs. Experimental (Nominal corner only)

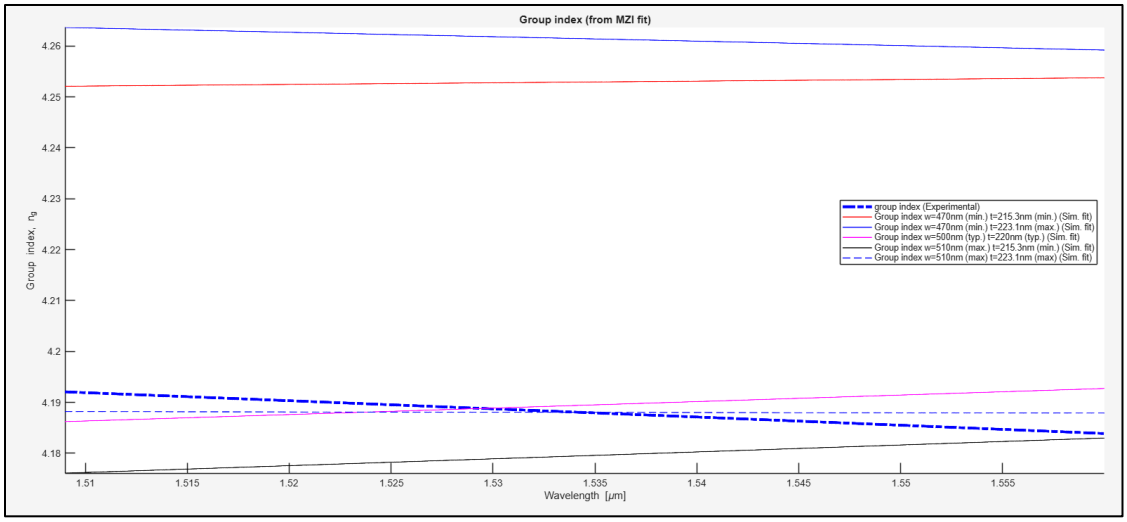

Figure 17 - 4: MZI 2 – Group index – Simulation Vs. Experimental (All corners)

MZI 3 - (ΔL = 114um, Predicted FSR (calculated) = 5nm)

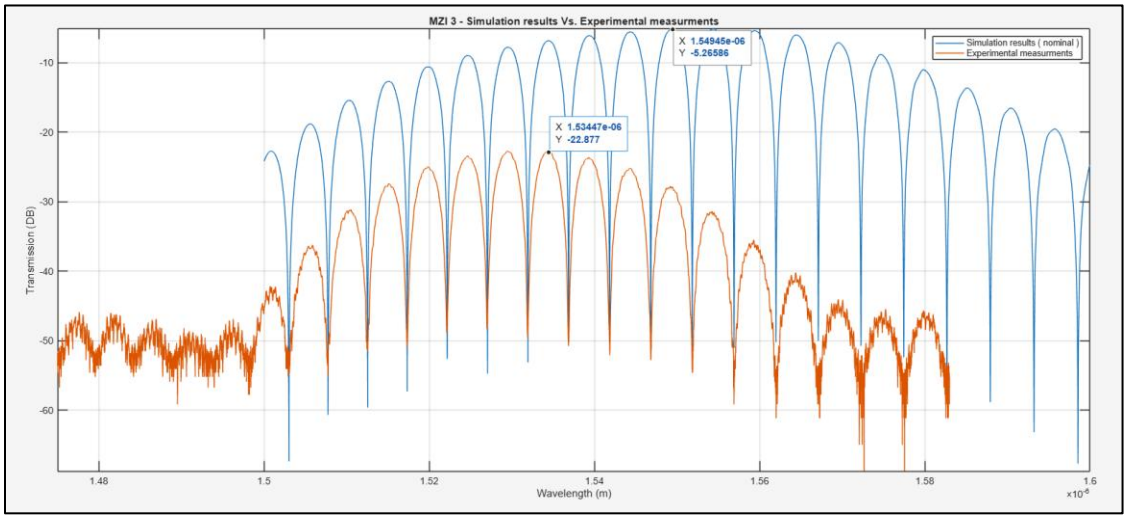

Figure 18 - 1: MZI 3 – Simulation (Nominal) Vs. Experimental data

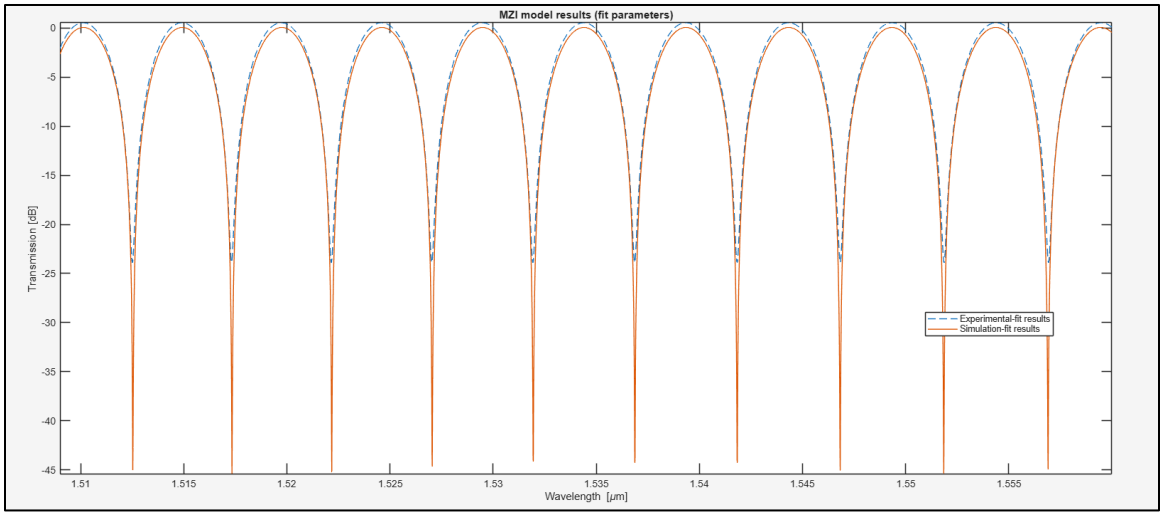

Figure 18 - 2: MZI 3 - MZI Transfer model fit – Simulation Vs. Experimental (Nominal corner only)

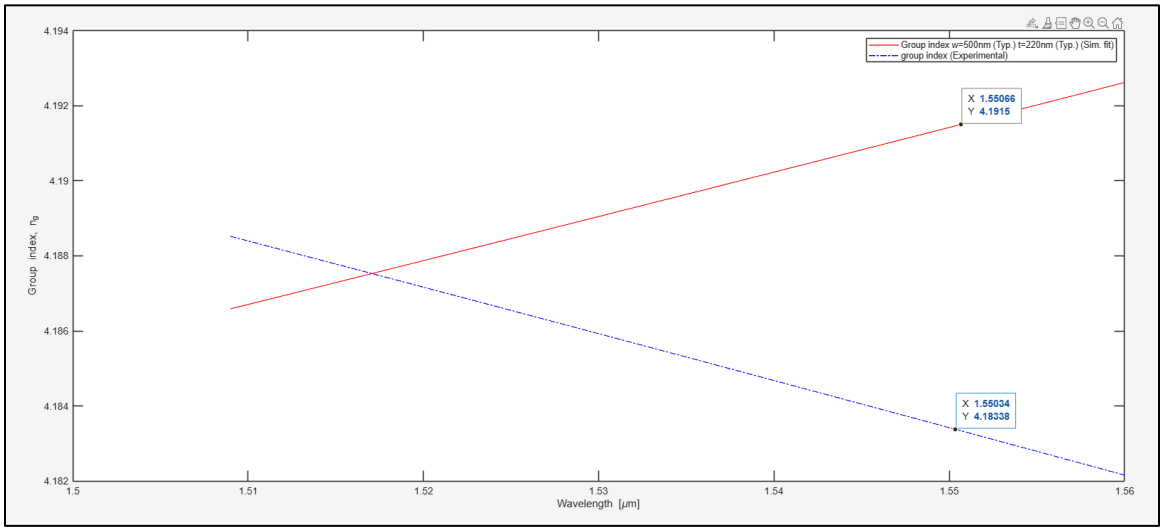

Figure 18 - 3: MZI 3 – Group index – Simulation Vs. Experimental (Nominal corner only)

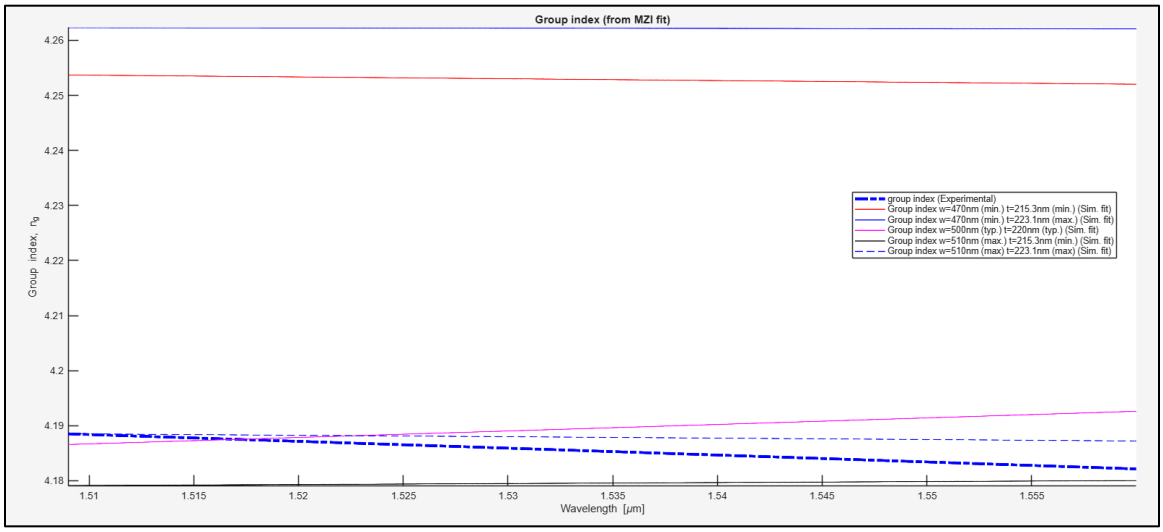

Figure 18 - 4: MZI 3 – Group index – Simulation Vs. Experimental (All corners)

MZI 4 - (ΔL = 229um, Predicted FSR (calculated) = 2.5nm)

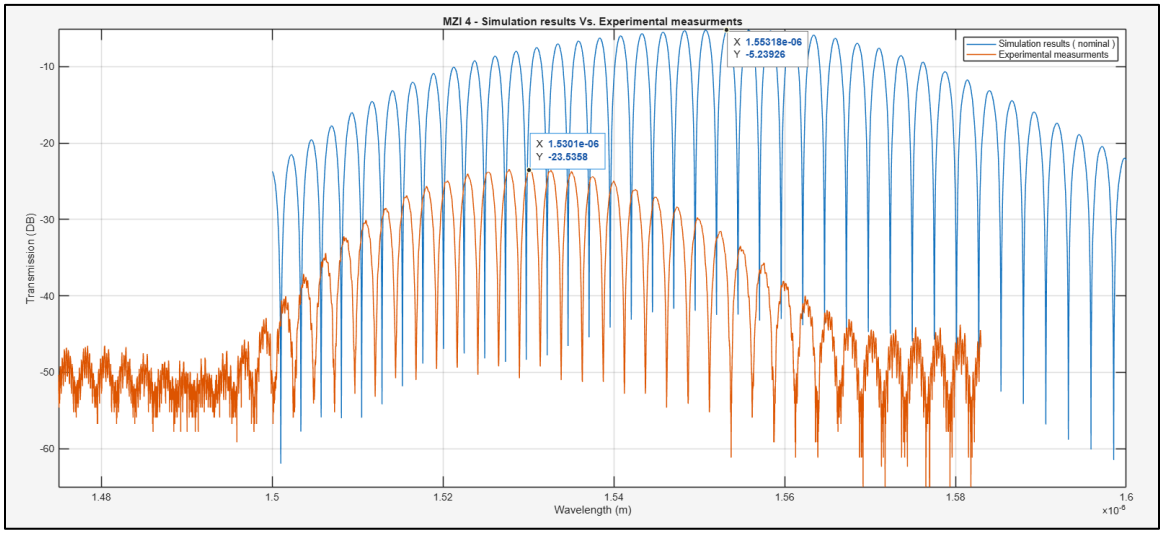

Figure 19 - 1: MZI 4 – Simulation (Nominal) Vs. Experimental data

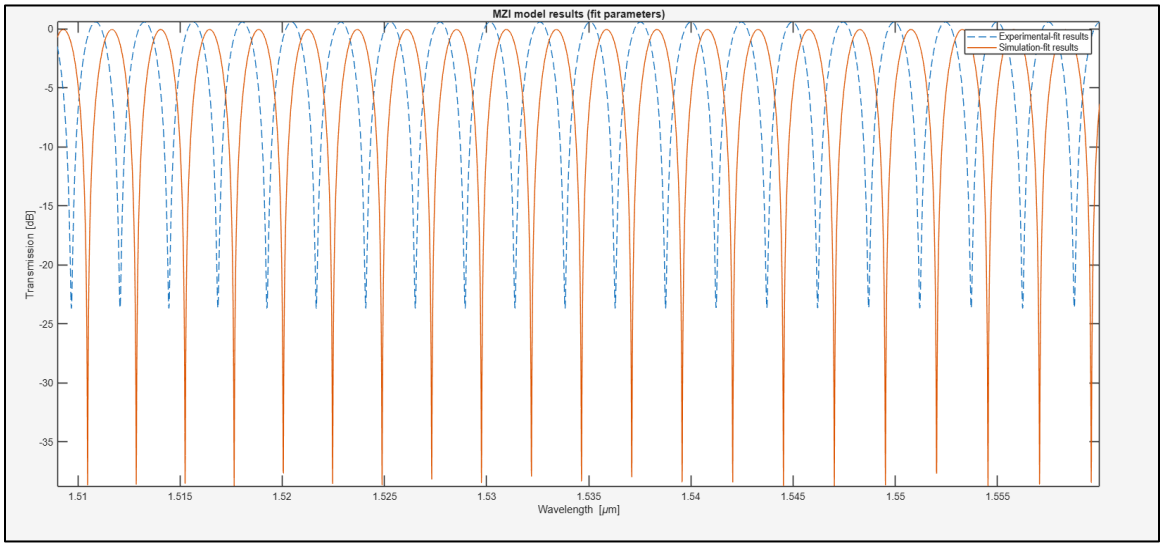

Figure 19 - 2: MZI 4 - MZI Transfer model fit – Simulation Vs. Experimental (Nominal corner only)

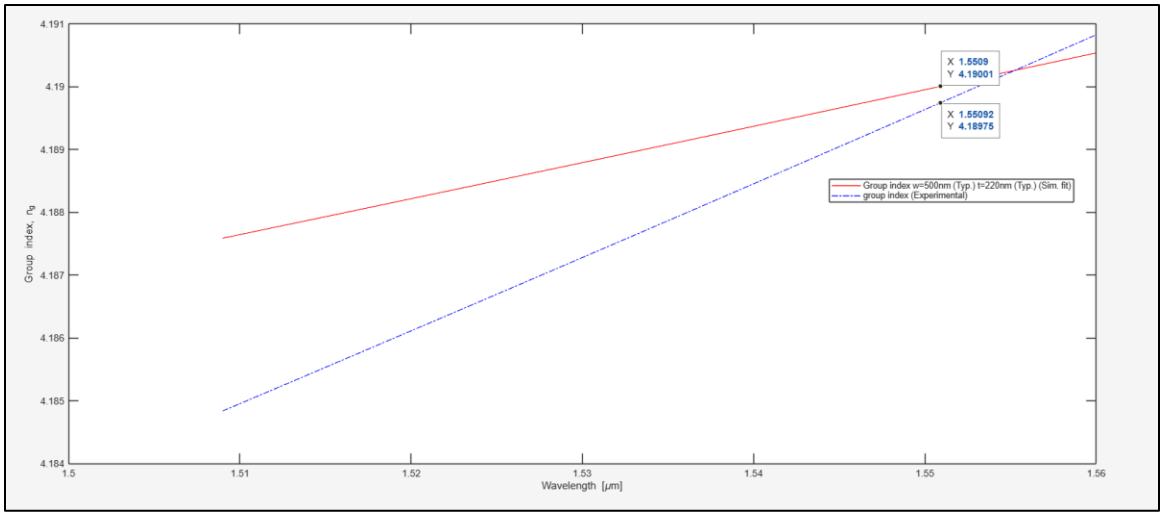

Figure 19 - 3: MZI 4 – Group index – Simulation Vs. Experimental (Nominal corner only)

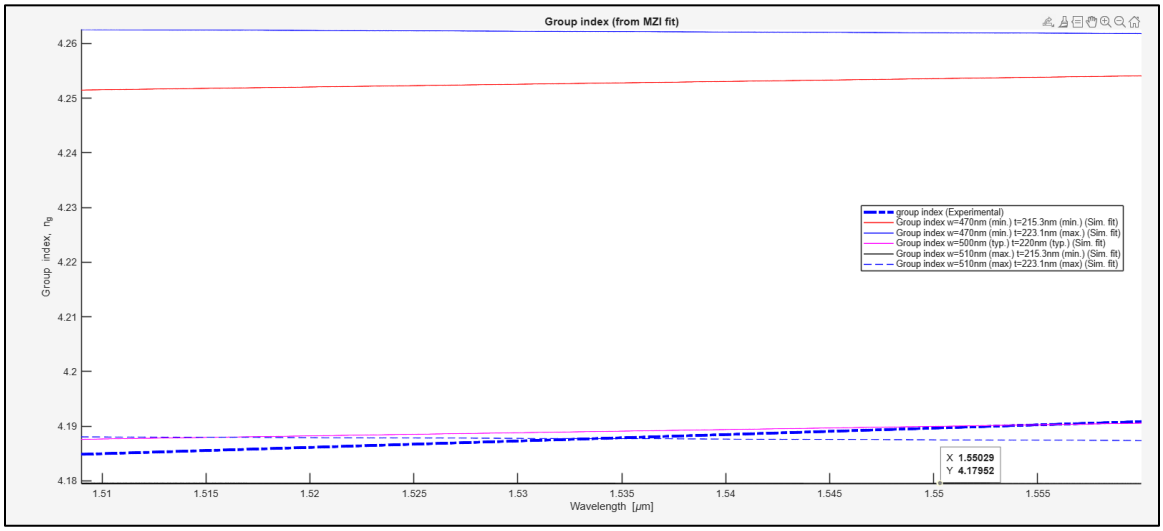

Figure 19 - 4: MZI 4 – Group index – Simulation Vs. Experimental (All corners)

MZI 5 - (ΔL = 114um, Predicted FSR (calculated) = 5nm)

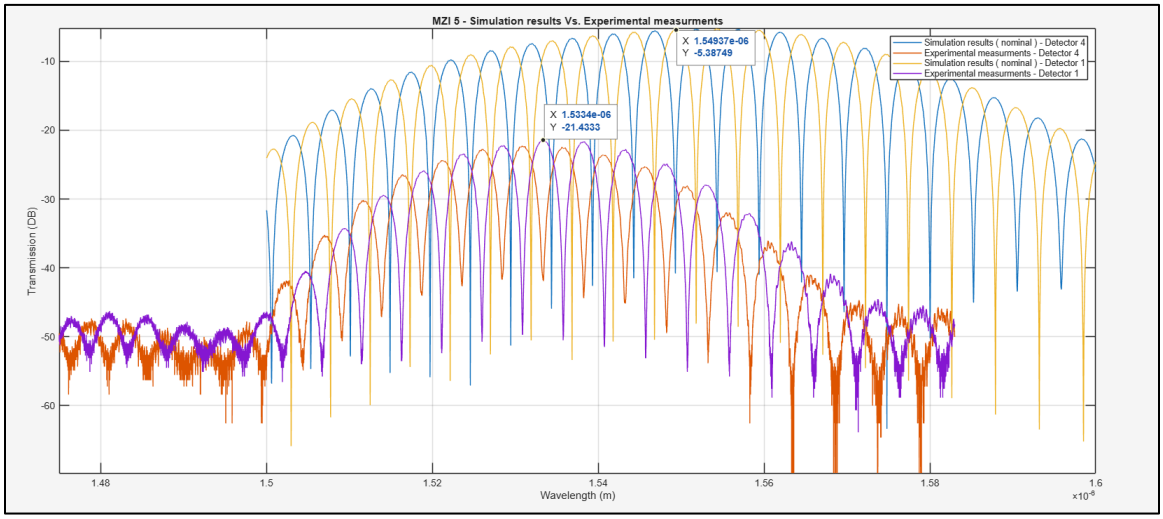

Figure 19 - 1: MZI 5 – Simulation (Nominal) Vs. Experimental data

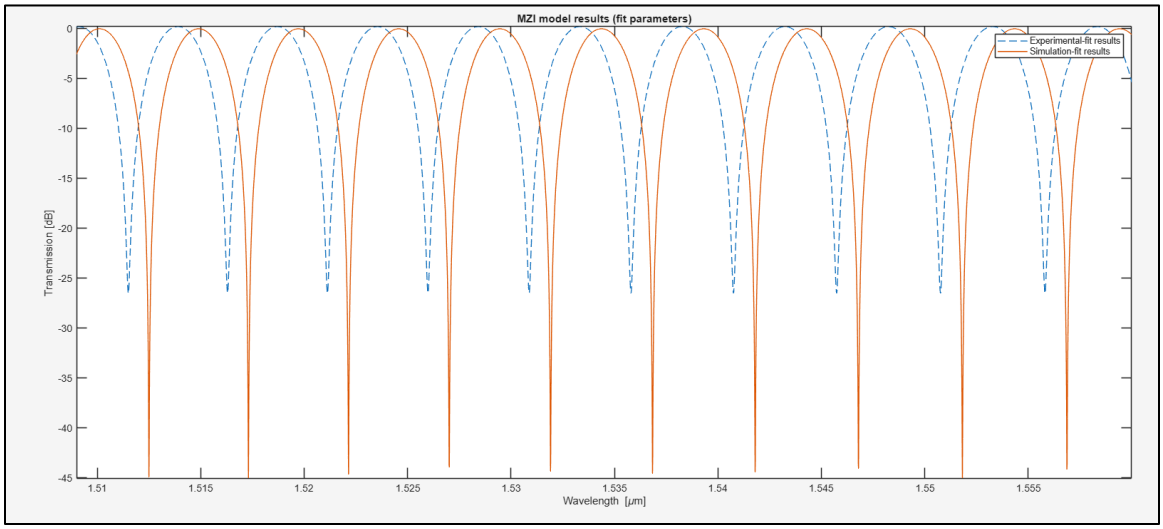

Figure 19 - 2: MZI 5 (Detector 1 - TOP GC) - MZI Transfer model fit – Simulation Vs. Experimental (Nominal corner only)

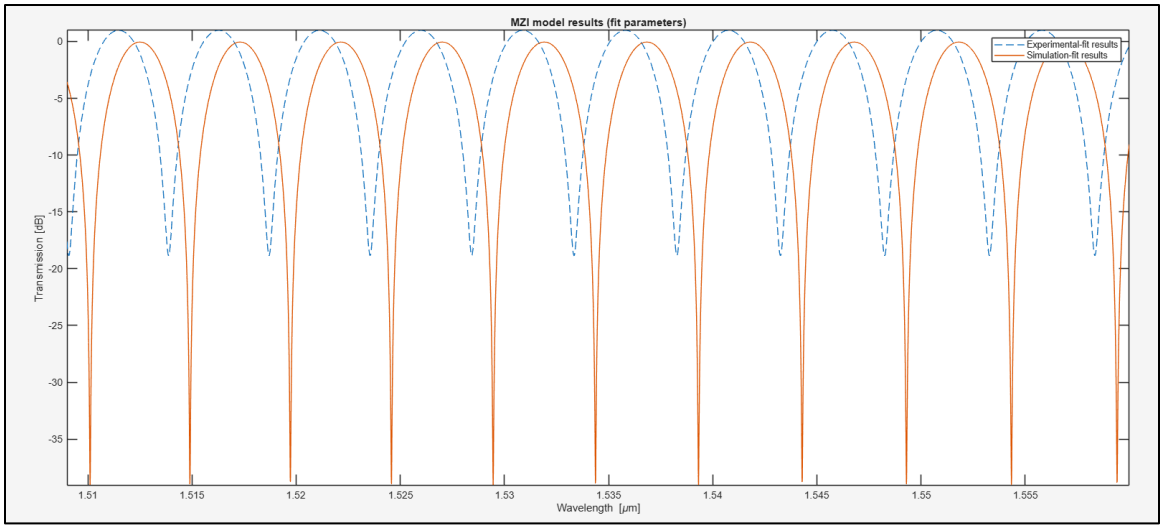

Figure 19 - 3: MZI 5 (Detector 4 - BOTTOM GC) - MZI Transfer model fit – Simulation Vs. Experimental (Nominal corner only)

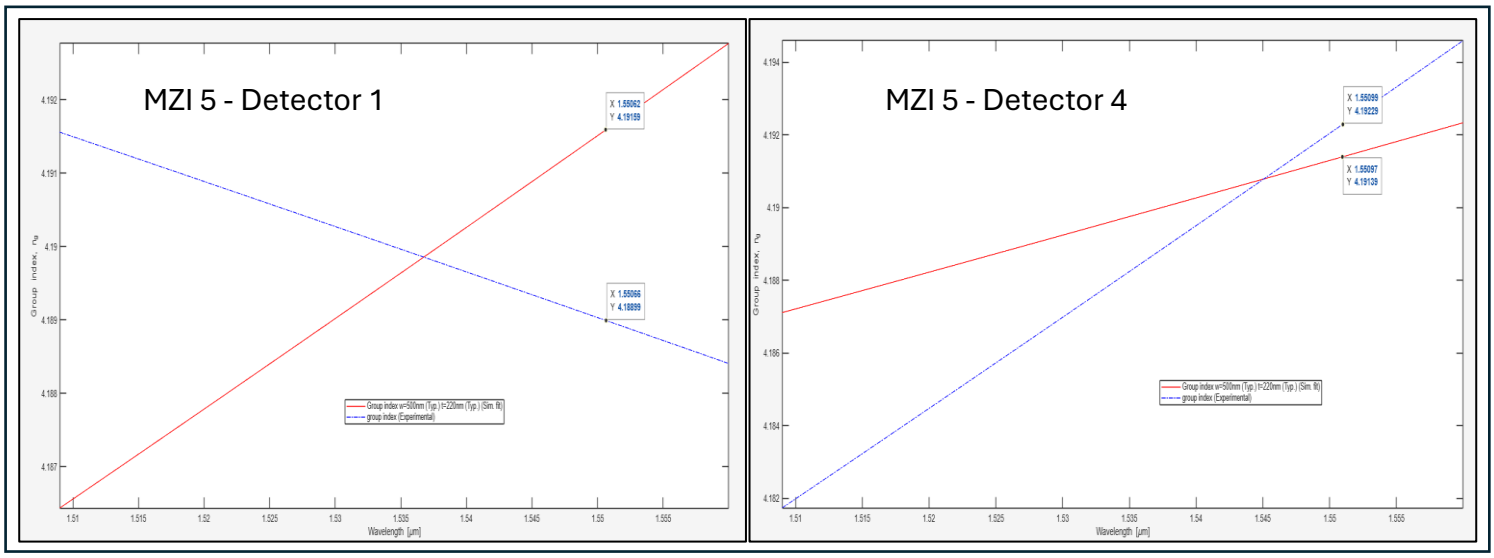

Figure 19 - 4: MZI 5 – Group index – Simulation Vs. Experimental (Nominal corner only)

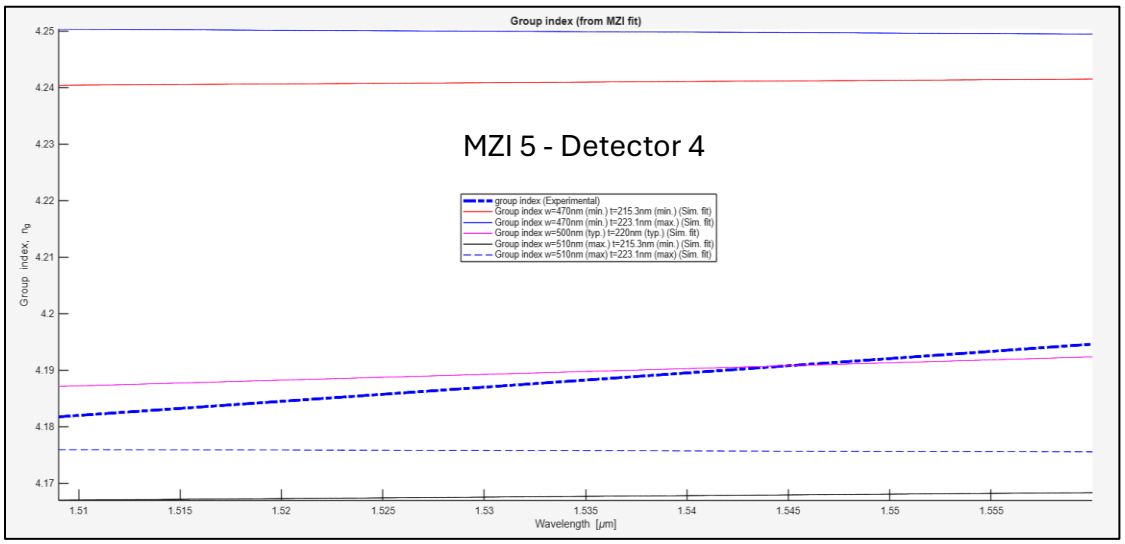

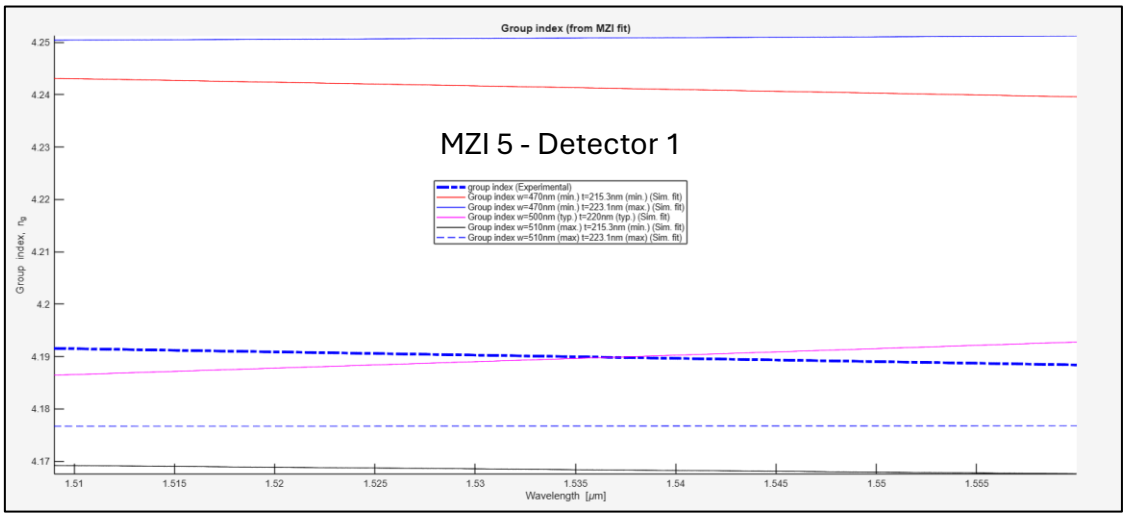

Figure 19 - 5: MZI 5 – Group index – Simulation Vs. Experimental (All corners)

Summary

This report focusses in two fundamental parameters of IMZI – FSR and Group index. It describes the data analysis flow of extracting these parameters from experimental results and compare it to simulation results.

The experimental result shows a very good compatibility to simulation result. According to group index plots of all corners, the experimental results are within corners range and shows low discrepancies with nominal corner (Width=500nm, Thickness=220nm).

The following table summarizes the results of both experimental and simulation for different structures of IMZI:

		FSR			Group index				
Layout cell name	ΔL (um)	FSR (nm) (Predicted) (Calculated with approximate n_g = 4.2)	FSR (nm) (Nominal simulation) (@ λ = 1550nm)	FSR (nm) (Experimental) (@ λ = 1530nm)	Group index (Corner simulation) @1550nm			Group index (Experimental) (@ λ = 1550nm)	Sim./Exp. discrepancy (%) (Relative to nominal value)
					MIN.	NOM.	MAX.		
IMZI_Y-Branch_1	38	15	14.81	14.304	4.1796	4.20358	4.26209	4.20524	0.039490149
IMZI_Y_Branch_2	57	10	9.88	9.888				4.18543	0.431774821
IMZI_Y_Branch_3	114	5	4.95	4.952				4.18338	0.480542775
IMZI_Y_Branch_4	229	2.5	2.47	2.472				4.18975	0.329005276
IMZI_BDC_SP_5 (GC Top)	114	5	4.93	4.944				4.18899	0.347085104
IMZI_BDC_SP_5 (GC Bottom)			4.95	4.936				4.19229	0.268580591

Table 4: FSR/Group index data analysis summary

SUMMARY OF THE FABRICATION DESCRIPTION:

Fabricated is performed at one or more of these: Applied Nanotools and Washington Nanofabrication Facility. The following are the process descriptions.

Applied Nanotools, Inc. NanoSOI process:

The photonic devices were fabricated using the NanoSOI MPW fabrication process by Applied Nanotools Inc. (http://www.appliednt.com/nanosoi; Edmonton, Canada) which is based on direct-write 100 keV electron beam lithography technology. Silicon-on-insulator wafers of 200 mm diameter, 220 nm device thickness and 2 µm buffer oxide thickness are used as the base material for the fabrication. The wafer was pre-diced into square substrates with dimensions of 25x25 mm, and lines were scribed into the substrate backsides to facilitate easy separation into smaller chips once fabrication was complete. After an initial wafer clean using piranha solution (3:1 H2SO4:H2O2) for 15 minutes and water/IPA rinse, hydrogen silsesquioxane (HSQ) resist was spin-coated onto the substrate and heated to evaporate the solvent. The photonic devices were patterned using a JEOL JBX-8100FS electron beam instrument at The University of British Columbia. The exposure dosage of the design was corrected for proximity effects that result from the backscatter of electrons from exposure of nearby features. Shape writing order was optimized for efficient patterning and minimal beam drift. After the e-beam exposure and subsequent development with a tetramethylammonium sulfate (TMAH) solution, the devices were inspected optically for residues and/or defects. The chips were then mounted on a 4" handle wafer and underwent an anisotropic ICP-RIE etch process using chlorine after qualification of the etch rate. The resist was removed from the surface of the devices using a 10:1 buffer oxide wet etch, and the devices were inspected using a scanning electron microscope (SEM) to verify patterning and etch quality. A 2.2 µm oxide cladding was deposited using a plasma-enhanced chemical vapour deposition (PECVD) process based on tetraethyl orthosilicate (TEOS) at 300ºC. Reflectrometry measurements were performed throughout the process to verify the device layer, buffer oxide and cladding thicknesses before delivery.

Washington Nanofabrication Facility (WNF) silicon photonics process

The devices were fabricated using 100 keV Electron Beam Lithography [1]. The fabrication used silicon-on-insulator wafer with 220 nm thick silicon on 3 µm thick silicon dioxide. The substrates were 25 mm squares diced from 150 mm wafers. After a solvent rinse and hot-plate dehydration bake, hydrogen silsesquioxane resist (HSQ, Dow-Corning XP-1541-006) was spin-coated at 4000 rpm, then hotplate baked at 80 °C for 4 minutes. Electron beam lithography was performed using a JEOL JBX-6300FS system operated at 100 keV energy, 8 nA beam current, and 500 µm exposure field size. The machine grid used for shape placement was 1 nm, while the beam stepping grid, the

spacing between dwell points during the shape writing, was 6 nm. An exposure dose of 2800 μC/cm2 was used. The resist was developed by immersion in 25% tetramethylammonium hydroxide for 4 minutes, followed by a flowing deionized water rinse for 60 s, an isopropanol rinse for 10 s, and then blown dry with nitrogen. The silicon was removed from unexposed areas using inductively coupled plasma etching in an Oxford Plasmalab System 100, with a chlorine gas flow of 20 sccm, pressure of 12 mT, ICP power of 800 W, bias power of 40 W, and a platen temperature of 20 °C, resulting in a bias voltage of 185 V. During etching, chips were mounted on a 100 mm silicon carrier wafer using perfluoropolyether vacuum oil. Cladding oxide was deposited using plasma enhanced chemical vapor deposition (PECVD) in an Oxford Plasmalab System 100 with a silane (SiH4) flow of 13.0 sccm, nitrous oxide (N2O) flow of 1000.0 sccm, high-purity nitrogen (N2) flow of 500.0 sccm, pressure at 1400mT, high-frequency RF power of 120W, and a platen temperature of 350C. During deposition, chips rest directly on a silicon carrier wafer and are buffered by silicon pieces on all sides to aid uniformity.

Measurement description:

To characterize the devices, a custom-built automated test setup [2, 6] with automated control software written in Python was used [3]. An Agilent 81600B tunable laser was used as the input source and Agilent 81635A optical power sensors as the output detectors. The wavelength was swept from 1500 to 1600 nm in 10 pm steps. A polarization maintaining (PM) fibre was used to maintain the polarization state of the light, to couple the TE polarization into the grating couplers [4]. A 90º rotation was used to inject light into the TM grating couplers [4]. A polarization maintaining fibre array was used to couple light in/out of the chip [5].

Acknowledgments:

I acknowledge the edX UBCx Phot1x Silicon Photonics Design, Fabrication and Data Analysis course, which is supported by the Natural Sciences and Engineering Research Council of Canada (NSERC) Silicon Electronic-Photonic Integrated Circuits (SiEPIC) Program. The devices were fabricated by Richard Bojko at the University of Washington Washington Nanofabrication Facility, part of the National Science Foundation's National Nanotechnology Infrastructure Network (NNIN), and Cameron Horvath at Applied Nanotools, Inc. Omid Esmaeeli performed the measurements at The University of British Columbia. We acknowledge Lumerical Solutions, Inc., Mathworks, Mentor Graphics, Python, and KLayout for the design software.

References:

[1] R. J. Bojko, J. Li, L. He, T. Baehr-Jones, M. Hochberg, and Y. Aida, "Electron beam lithography writing strategies for low loss, high confinement silicon optical waveguides," J. Vacuum Sci. Technol. B 29, 06F309 (2011)

[2] Lukas Chrostowski, Michael Hochberg, chapter 12 in "Silicon Photonics Design: From Devices to Systems", Cambridge University Press, 2015

[3] http://siepic.ubc.ca/probestation, using Python code developed by Michael Caverley.

[4] Yun Wang, Xu Wang, Jonas Flueckiger, Han Yun, Wei Shi, Richard Bojko, Nicolas A. F. Jaeger, Lukas Chrostowski, "Focusing sub-wavelength grating couplers with low back reflections for rapid prototyping of silicon photonic circuits", Optics Express Vol. 22, Issue 17, pp. 20652-20662 (2014) doi: 10.1364/OE.22.020652

[5] www.plcconnections.com, PLC Connections, Columbus OH, USA.

[6] http://mapleleafphotonics.com, Maple Leaf Photonics, Seattle WA, USA.